

A review of flexible halide perovskite solar cells towards scalable manufacturing and environmental sustainability

Melissa Davis and Zhibin Yu†

Department of Industrial and Manufacturing Engineering, High-Performance Materials Institute, FAMU-FSU College of Engineering, Florida State University, Florida 32310, USA

Abstract: The perovskite material has many superb qualities which allow for its remarkable success as solar cells; flexibility is an emerging field for this technology. To encourage commercialization of flexible perovskite solar cells, two main areas are of focus: mitigation of stability issues and adaptation of production to flexible substrates. An in-depth report on stability concerns and solutions follows with a focus on Ruddlesden-Popper perovskites. Roll to roll processing of devices is desired to further reduce costs, so a review of flexible devices and their production methods follows as well. The final focus is on the sustainability of perovskite solar cell devices where recycling methods and holistic environmental impacts of devices are done.

Key words: material; thin film; diode

Citation: M Davis and Z B Yu, A review of flexible halide perovskite solar cells towards scalable manufacturing and environmental sustainability[J]. *J. Semicond.*, 2020, 41(4), 041603. <http://doi.org/10.1088/1674-4926/41/4/041603>

1. Introduction

Halide perovskites have quickly shown success as promising new photovoltaic materials. The record efficiency from such materials has reached 25.2% which rivals that of single junction silicon, the leading commercialized material^[1]. Moving forward, a promising direction of perovskite solar cells, or PSCs, is their ability to be manufactured on flexible substrates; so, scalable manufacturing of perovskite solar panels can be readily achieved at a low cost. In addition, flexible PSC would also increase the number of applications. Due to the lower weight, they become advantageous for shipping and installation and other weight sensitive occasions. Also, flexible modules can be applied on angular surfaces.

Although perovskite solar cells have shown impressive efficiencies, they have accompanying challenges. Three of the most noted challenges for rigid PSCs are hysteresis, stability, and the use of lead. These disadvantages also affect flexible devices. To encourage commercialization, these factors need solutions. Therefore, for this review on flexible perovskite solar cells, additional focus will also be placed on these challenges. We will begin with an overview of the properties of the perovskite material followed by a section on hysteresis. The following section will address the instability seen in perovskite devices and proposed solutions. A focus on Ruddlesden-Popper perovskite solar cells will be discussed as a solution to the perovskite material's instability. Commercialization is the focus of the final two sections where upscaling is discussed with a review on flexible PSCs and roll-to-roll PSCs. The final section relates to the environmental impact of PSCs where the focus is on lead and a cradle to grave assessment of the devices.

2. Basic properties of halide perovskites

The perovskite material has many unique properties which promotes its ability to be an effective solar cell material. Perovskite solar cells utilize the perovskite crystalline structure. It can be found in nature; however, in solar cells, the crystal is synthesized in a laboratory setting. The general formula is ABX_3 where 'A' and 'B' are cations and X is an anion. The perovskite crystal structure is cubic where 'B' is surrounded by an octahedron of X anions (Fig. 1)^[2]. Various anions and cations can be selected for each position. The 'A' anion is typically divalent and commonly used compounds are methylammonium, MA or CH_3NH_3 , formamidinium, FA or $CH(NH_2)_2$, and cesium, Cs^[3]. The 'B' anion is typically either lead or tin, while the 'X' position has many options with halogens most commonly used: iodide, chloride, or bromide.

Selection of ions has a direct impact on the geometric shape of the unit cell. The Goldschmidt tolerance factor, t , can be calculated to determine if the unit cell will remain cubic and stable. It is calculated through the ionic radii of each ion and is as follows:

$$t = (r_A + r_X) / \sqrt{2}(r_B + r_X), \quad (1)$$

where r_A , r_B , r_X are the ionic radii of 'A', 'B', and 'X' ions. If the tolerance factor is less than one, the cubic structure will have distortion. The tolerance factor can be used to determine if selection of ions can create a formable perovskite structure^[5]. For alkali metal halide perovskites, the tolerance must remain within bounds of 0.813 to 1.107; therefore, a tolerance factor below one can still create a perovskite structure so long as it remains within the range.

Ion selection also has a direct impact on the bandgap of the material^[6]. One of the benefits of the perovskite material is its ability to tune its bandgap. If the ion radius of 'X' increases while 'A' and 'B' ions remain the same, the bandgap of the perovskite decreases^[7]. This relationship is seen with

Correspondence to: Z B Yu, zyu@fsu.edu

Received 30 DECEMBER 2019; Revised 10 MARCH 2020.

©2020 Chinese Institute of Electronics

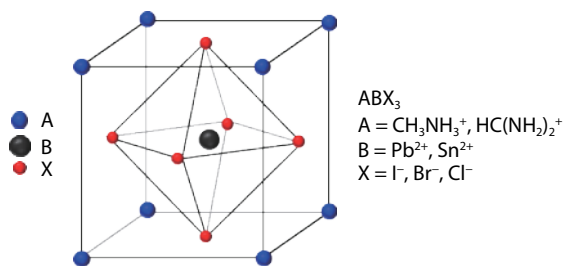


Fig. 1. (Color online) Crystal structure diagram for the perovskite material^[4].

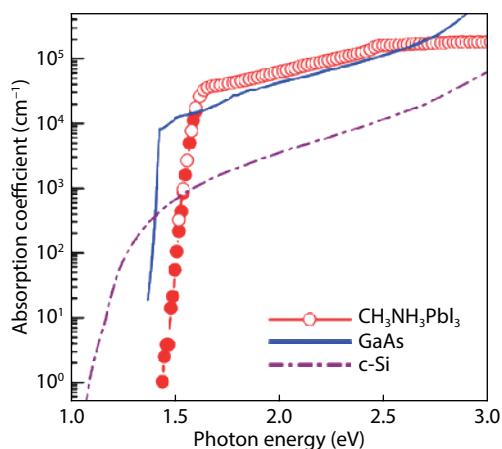


Fig. 2. (Color online) Absorption coefficients over photon energy for perovskite, GaAs, and single crystal silicon^[8].

the bandgap of 1.5 eV for MAPbI₃ and 2.8 eV for MAPbCl₃. The increase in bandgap is due to chlorine's smaller ionic size. The ions in every position can be swapped to further manipulate the bandgap or elicit various benefits. For example, tin is commonly used to replace toxic lead. Nonetheless, the most used perovskite for solar cells is MAPbI₃.

The perovskite material also has a superb absorption coefficient. An explanation for this property is its direct bandgap which minimizes loss of photon energy. Absorption coefficients are found by measuring light absorption of the material over a range of photon energies. MAPbI₃ perovskites have a graph that is seen in Fig. 2. A sharp trend is seen at the bandgap near 1.5 eV; therefore, photons with energy at or above 1.5 eV have a high likelihood of being absorbed. A nearly perpendicular line shows that perovskite solar cells have a direct bandgap and structural order. Silicon SCs have a slower gradient on the rising edge; this corresponds with an indirect bandgap and more prevalent structural disorder^[8]. The slope of the initial peak of absorption is related to the Urbach energy, or the sub-bandgap absorption edge. A sharp, nearly perpendicular line corresponds to a low Urbach energy where the material has minimal structural issues. A more gentle slope has a large Urbach energy that shows a material with more structural issues^[9].

Another benefit of the perovskite material's high absorption coefficient is ability to absorb photons with a thin layer. The coefficient varies over the range of photon energies and corresponding wavelengths. For MAPbI₃ perovskite SCs, an absorption coefficient of $0.5 \times 10^4 \text{ cm}^{-1}$ at 700 nm was calculated^[8]. This corresponds to a penetration depth of 2 μm . Therefore, incoming light of wavelength 700 nm or lower can be absorbed with a perovskite layer of thickness 2 μm ^[2]. A

thin active layer is desirable to minimize material use. Once light is absorbed, charge transport properties are key to ensure charge extraction. To ensure ideal extraction, diffusion lengths must be greater than the absorption depth^[10, 11]. Diffusion lengths can differ with halide choice; however, perovskite's have consistently longer diffusion lengths than other third generation technologies^[12].

3. Current challenges in perovskite solar cells

3.1. Hysteresis

Hysteresis is the phenomenon of differing efficiencies due to the scan direction of the testing equipment. A perovskite solar cell with hysteresis has two different results based on the scan direction and other factors. In addition, a PSC with hysteresis has different results due to previous tests; in other words, it has memory. Scan speed is another factor which affects hysteresis. Snaith *et al.* declares that fast scanning shows less hysteresis over slow scanning while other researchers formulate the inverse^[13, 14]. See Fig. 3 for a visual depiction of hysteresis in testing of PSC.

Two main causes for hysteresis have emerged: device materials and structure, and defects within the crystal. The former cause, device materials and structure, correlates to research which shows that the hysteresis effect is reduced in perovskite solar cells with an inverted structure^[16]. With capacitance measurements, or the build-up of charges within PSCs, Kim *et al.* discovered that replacing commonly used conventional layers, TiO₂ and spiro-MeOTAD, with inverted layers, PEDOT:PSS and PCBM, the capacitive effects decreased^[17]. This decreases hysteresis and protects the PSCs from degradation that occurs from capacitive effects.

The other main cause of hysteresis is believed to be due to defects within the crystalline structure^[18]. The defects allow for ions to migrate and can also trap charges within the structure. Pacification of grain boundaries has been shown with fullerenes such as PCBM. When PCBM is applied a top of the perovskite, it seeps into the grain boundaries and pacifies the traps within the boundary^[14]. This is an additional explanation for inverted PSC's decrease in hysteresis, as inverted PSC commonly utilize PCBM. Another issue within the crystal is the movement of ions. Additives have been researched to combat this problem. Son *et al.* included potassium iodide within their perovskite layer. The potassium prevented the movement of iodide within the crystal which decreased hysteresis^[19].

While hysteresis is a problem in PSC, it can be minimized and removed through reducing defects and other trap states. It is still a continuing concern that plagues some PSCs; however, hysteresis is not a major concern for current record perovskite solar cells. Currently, the greatest issue plaguing perovskite solar cells is their short lifetime and instability.

3.2. Stability

Perovskite solar cells to demonstrate short lifetimes due to instability from various factors. The main challenge of perovskite solar cells is their stability. PSC cells have efficiencies which decrease over time due to degradation. This trend is not desired for commercialization and the decreasing efficiency is mainly caused by degradation of the perovskite layer. The four most common methods for perovskite film degrad-

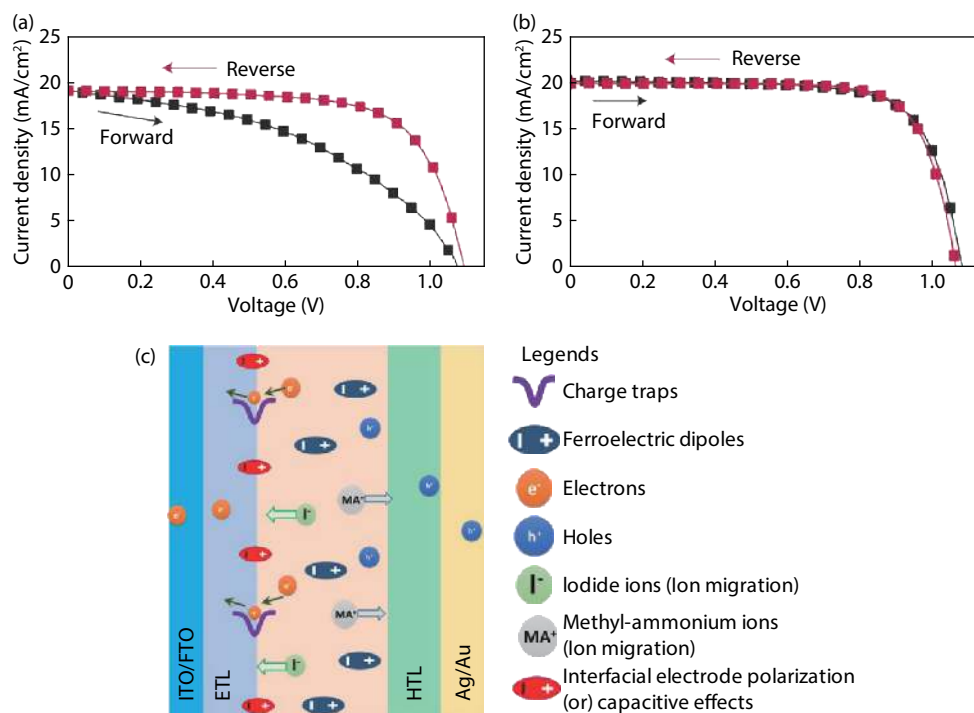


Fig. 3. (Color online) Current–voltage performance of a PSC with (a) hysteresis properties and (b) no hysteresis properties. (c) Schematic diagram denoting potential causes of hysteresis in a PSC^[15].

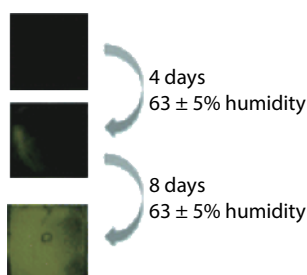
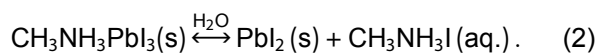


Fig. 4. (Color online) Time lapse of perovskite film degradation due to humidity^[22].

ation is through moisture, oxygen, UV light, and heat. The perovskite material is sensitive to its environment during fabrication. Most perovskite layers are deposited and annealed within a controlled environment such as a nitrogen or argon filled glovebox. With a glovebox, the effect of the previously stated factors is significantly decreased.

The greatest threat to the perovskite structure, as well as the most studied, is moisture and humidity. Water is a strong enemy of perovskite films. Moisture easily breaks down the perovskite into its precursors^[20]. For MAPbI₃, it reverts the perovskite back into lead iodide and methylammonium iodide as seen in Eq. (2). This can easily be seen visually when the black or dark brown perovskite films change into a yellow film as seen in Fig. 4^[21]. Yellow specifies that the lead iodide has been released from the perovskite structure.



One common method to combat the ingress of moisture is to increase the crystallinity of the perovskite structure. Noh *et al.* discovered that including a fraction of bromide into the perovskite structure shrinks the lattice to inhibit the en-

trance of water^[23]. Halide replacement is another solution; researchers have created PSCs with thiocyanate, or SCN, as its halide. It is formulated that the SCN has a stronger bond with the lead ion thus making it harder for moisture to degrade the films^[24, 25].

The second factor which most commonly affects perovskite films is oxygen. It is important to note that oxygen can only damage the film while the cell is illuminated^[26, 27]. The need for both illumination and oxygen is seen in Fig. 5. Oxidation occurs in the film when oxygen diffuses within the crystal through iodide vacancies. Once diffused, oxygen will trap electrons to create a highly reactive superoxide which then reacts with the 'A' ion to create water^[28]. This water then degrades the film as described previously. Saidaminov *et al.* discovered that adding cadmium in the perovskite aids in the reduction of iodide vacancies^[29]. Cadmium doping is believed to alleviate strain within the local lattice. Another method to reduce degradation is with the use of less acidic 'A' cations such as cesium or formamidinium^[21].

UV light can also degrade the film. PSCs with a layer of TiO₂ are especially vulnerable to degradation due to UV light^[30]. TiO₂ is easily oxidized in UV light. Its result, a superoxide, then reacts with the perovskite as previously stated in the oxygen degradation section. To mitigate this problem, a UV filter can be added or TiO₂ can be replaced. Ouafi *et al.* incorporated bromide into the halide and was successful in reducing the effect of UV light^[31]. Researchers showed that methylammonium perovskites with 20% or more bromide maintain stability during UV irradiation (Fig. 6).

The final degradation method is thermal irradiation or heat. High temperatures can cause the perovskite structure to change its phase. With regards to heat degradation, the 'A' ion has the greatest effect on thermal stability. The common PSC utilizes MAI which is more reactive than other 'A' ions

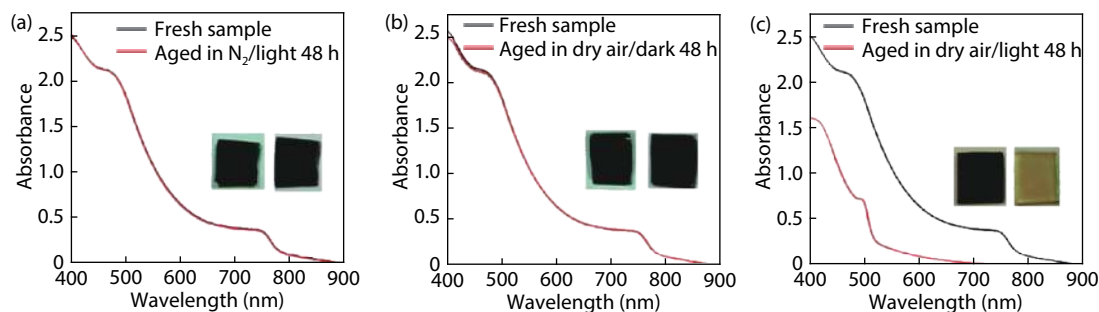


Fig. 5. (Color online) Stability depicted by change in absorption of perovskite films for two days in (a) illuminated, nitrogen atmosphere, (b) dark, nitrogen atmosphere, (c) illuminated, ambient atmosphere^[27].

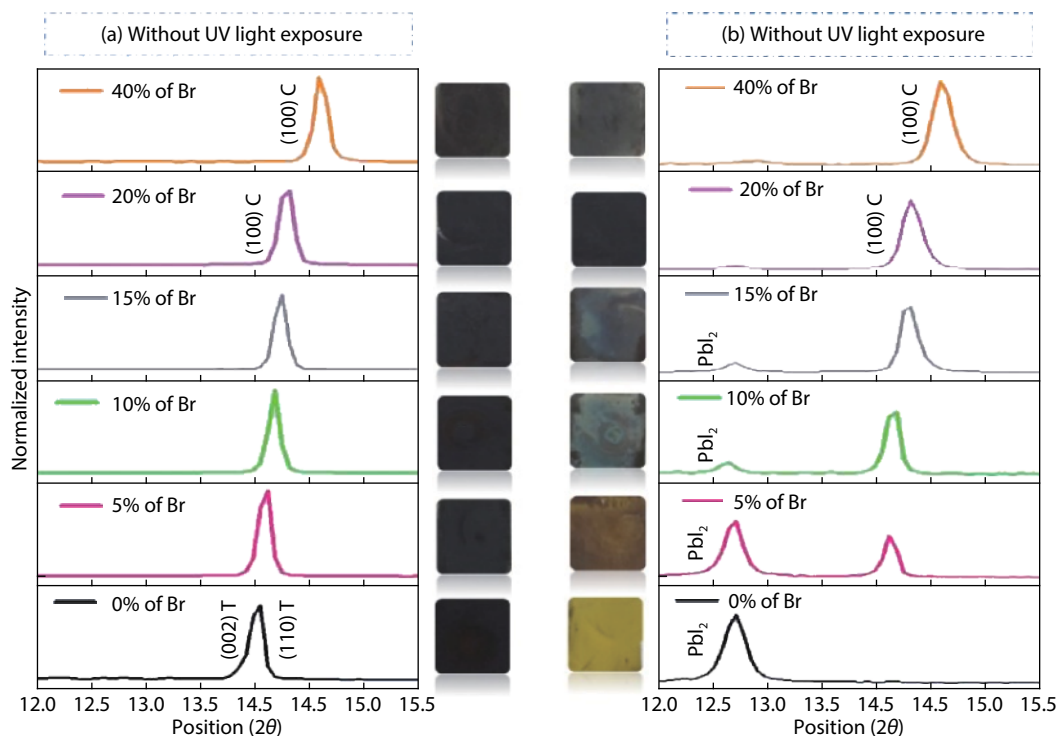


Fig. 6. (Color online) Effect of UV light stability due to percentage of bromide included in PSC^[31].

such as Cs or FAI^[21]. A solution to mitigate the effects of heat is with the addition of a layer of graphene, which has excellent thermal properties^[32].

Stability is a major concern for the commercialization prospects of PSCs. The two leading sources of instability are moisture and oxygen. Perovskite degradation is greatly fueled by the generation of water within the perovskite which quickly breaks down the two components of the structure. Methods to reduce this occurrence focus on creating a stronger crystalline lattice with compositional changes. A solution to the threat of degradation can be through encapsulation and the use of Ruddlesden-Popper perovskites.

3.2.1. Encapsulation

A method to reduce the hazard of lead and improve stability of PSC is through encapsulation. It is also a completely necessary step for commercialization. The most common methods to encapsulate solution processed solar cells is with a glass cover and epoxy. Encapsulation is key to protect the perovskite film from outer elements, as well as to protect the environment from chemical elements which may be detrimental to nature.

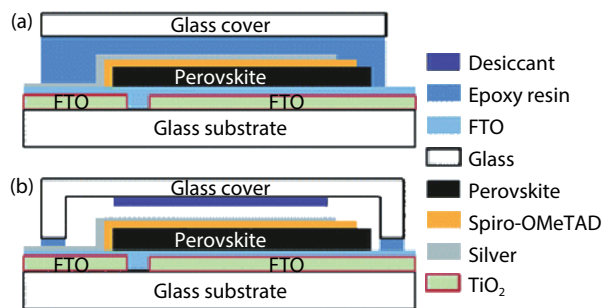


Fig. 7. (Color online) Encapsulation methods for PSCs (a) with a full covering of epoxy and (b) with a 'u'-shaped glass cover and a desiccant^[33].

The cell can be encapsulated by sandwiching the glass substrate with the layers between another flat glass slide and filling remaining space with an epoxy resin. Another option is to use a 'U' shaped glass cover with an internal desiccant. In this set-up, the epoxy resin is only used on the outer edges to create a complete seal between the bottom glass substrate and the upper glass cover^[33]. EVA, or ethylene vinyl acet-

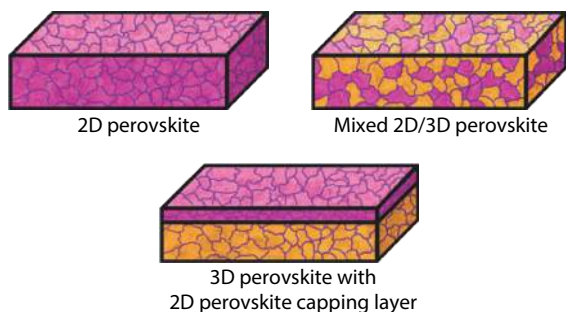


Fig. 8. (Color online) Three common examples of 2D perovskites as the active layer of PSCs^[38].

ate, is most commonly used as the epoxy resin. The former set-up was adopted from the encapsulation method that organic LEDs, or OLEDs, utilize as they are also moisture sensitive. Fig. 7 shows both encapsulation options.

3.2.2. Ruddlesden-Popper perovskite solar cells

Another method to improve perovskite solar cell's stability is the introduction of two-dimensional perovskite structures. Two-dimensional perovskite structures for solar cells are commonly large organic cations which grow in flat sheets. By nature, they are hydrophobic and slightly insulating^[34, 35]. They can be utilized in perovskite solar cells multiple ways. Solar cells can be made with an active material of pure 2D perovskites^[36]. Another method is placing a thin buffer/capping layer of 2D perovskites on top of the pure 3D layer^[35]. A final and the most commonly used method is to create a hybrid mixture of 2D and 3D perovskites^[37]. The three formulations can be seen in Fig. 8.

The ratio of 2D perovskite to 3D perovskite is key for the distinction between groups. If there is a small amount of 2D within the 3D perovskite, a mixed or passivated layer will be created. If there is a more similar ratio, such a one-part 2D perovskite to five parts 3D perovskite, then a periodic pattern will emerge. See Fig. 9 for a graphical description of some of the 2D material structure options.

The Ruddlesden-Popper perovskite structure is one type of the periodic patterns which can emerge. It is the most common and is seen when the 2D layers slice the 3D matrix within the [110] direction. Another type of perovskite structure is the Dion-Jacobson or DJ type. A main difference between the two is that DJ type perovskites are suited to wide-infrared range^[38]. While DJ perovskites do have a higher degree of crystallinity, RP type's smaller bandgap and ability to control thickness lend it to be more commonly be used for solar cells.

The Ruddlesden-Popper perovskite structure utilizes a layer structure with 2D and 3D structures intermixed in a periodic pattern. The distance between the 2D material is typically denoted by an ' n '. If the ' n ' is one, then there is one layer of 3D perovskite between each 2D layer. If the ' n ' is five, there are five rows of the 3D perovskite between each 2D layer. A pure 3D perovskite solar cell has an ' n ' of infinity; it has indefinite layers of the 3D perovskite with no 2D perovskite layers^[34, 39]. A visual example is seen in Fig. 10.

In addition to 2D perovskite's hydrophobic nature, the layered structure creates natural quantum wells which lead to more insulating behaviors^[41]. Therefore, Ruddlesden-Popper perovskites have tunable bandgaps with a manipulation of its ' n ' value. When the ' n ' value is lower, the bandgap of

the material is higher. While the exact bandgaps are unique to the chemical make-up, an increase in the amount of 2D layers leads to a higher bandgap. For MAPbI₃ perovskites, the bandgap of the pure material is 1.6 eV; therefore, layered perovskites with an ' n ' of 3 will have a higher bandgap such as 2.1 eV, which is less ideal^[39]. The ideal bandgap of a single-junction solar cell is 1.34 eV^[42]. While an increase in bandgap is not desired for some materials, the layered perovskite addresses a much more needed issue, its stability. By adding the 2D material, layered perovskite devices have a much-improved stability.

Material selection is key for Ruddlesden-Popper solar cells much like pure 3D perovskite solar cells. The general chemical structure for RPSCs is (RNH₃)₂A _{$n-1$} M _{n} X _{$3n+1$} where 'A' is an organic cation such as methylammonium, 'M' is lead or tin, and 'X' is typically a halogen^[43]. RNH₃ is the two-dimensional portion that is a spacer cation. 'R', 'B', and 'X' are the same commonly used chemicals such as methylammonium, lead, and a halide group^[41].

Processing of Ruddlesden-Popper perovskites

An issue with Ruddlesden-Popper, or RP, cells is that their periodic nature is not guaranteed to be consistent throughout the layer. While stoichiometry can control the ' n ' layers, layers of differing ' n ' values grow. Research has found that controlling the ' n ' layers to values between one and five allows for higher success in creating phase pure films^[41, 44]. Higher order ' n ' value RP films have layers with the stated ' n ' value, as well as values that are above and below the desired value. This leads research to be limited to ' n ' values less than seven if pure phases are desired.

Growth orientation is a key research focus. The crystallinity can grow parallel, perpendicular, or nonuniformly to the substrate (Fig. 11)^[45]. Vertical or perpendicular orientation is desired as it encourages generated charges to easily flow into the transport layers^[46]. If the 2D and 3D layers grow parallel to the substrate, charges can build up between the layers therefore encouraging hysteresis effects. The ability to store charge is due to the insulating nature of the spacing 2D ions.

Various processes have been discovered to change the growth orientation. One such way is utilizing a process called hot pressing or hot casting. Hot casting is when the substrate is preheated before the layer is applied with spin-coating. Most researchers heat their substrate to temperatures around 150 °C and then quickly move it to the spin coater. Another method to grow crystals out of plane is through the manipulation of solvents^[36]. Gao *et al.* balanced solvents DMSO and DMF in an equal ratio to form highly oriented films. Their work is seen in Fig. 12.

Another method to control growth orientation is through selection of spacing cations. There are nearly limitless options for 2D perovskite cations. The main benefits of utilizing a 2D cation is its ability to improve crystallinity and increase stability. Selection of cations is an optimization of the benefits. In addition, size or length of cations is useful. The length of the 2D spacer cations is directly related to the bandgap. Compounds with a longer chain length lead to films with higher bandgaps due to the insulating properties of long chains^[47].

Ruddlesden-Popper devices with PEA

In 2014, Smith *et al.* published work on one of the first

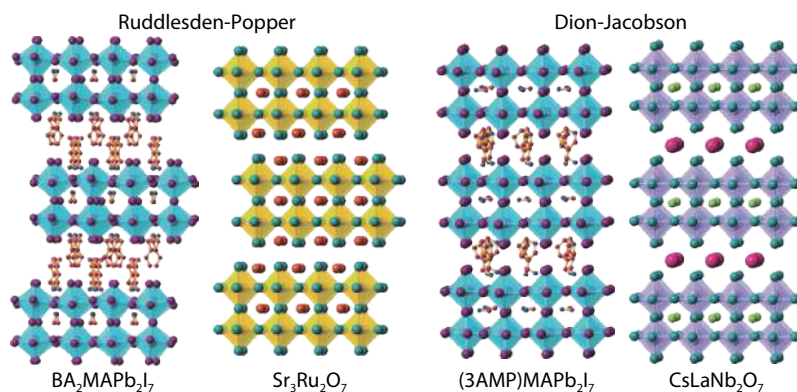


Fig. 9. (Color online) Crystal Structures of Ruddlesden-Popper and Dion-Jacobson perovskites^[38].

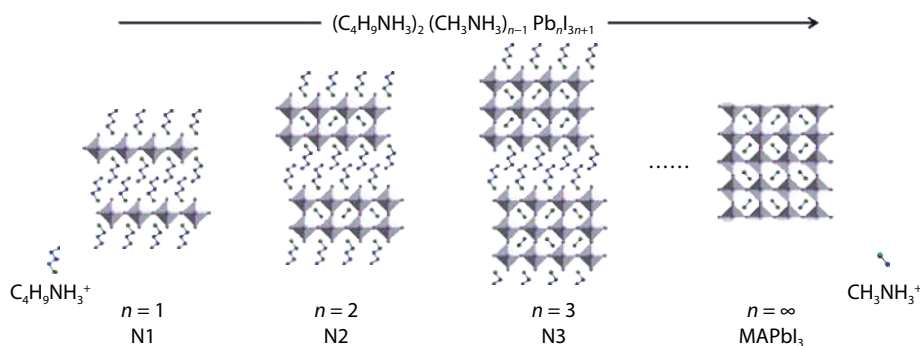


Fig. 10. (Color online) Crystal structure for Ruddlesden-Popper perovskites with increasing 'n' values^[40].

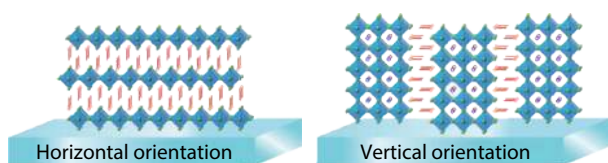


Fig. 11. (Color online) Growth orientations of Ruddlesden-Popper perovskites: horizontal and vertical^[38].

Ruddlesden-Popper PSCs. The 2D material was phenethyl ammonium or PEA and an efficiency of 4.73% was discovered^[39]. While the efficiency was lower than those of pure 3D PSCs, devices with PEA showed more stability and resistance to moisture. The full formula for PEA is as follows: $C_6H_5(CH_2)_2NH_3$ ^[39]. Recent work in 2019 by Gao developed a method to create PSCs with an efficiency of 12.29%^[36]. With solvent optimization and an 'n' value of five, researchers were able to create perpendicular, highly ordered PSC.

Further improvement of PEA was published in 2019 by Shi *et al.*^[48]. Researchers replaced hydrogen within PEA with fluorine to increase the hydrophobic nature of the Ruddlesden-Popper perovskite solar cells, or RPPSCs. An efficiency of 17.3% was shown which drastically improved the previous efficiency of PEA at 12.29%. Devices were made with simple spin coating procedures without hot casting methods.

Ruddlesden-Popper devices with BA

The most commonly used A' compound is $CH_3(CH_2)_3NH_3$ or n-butylammonium. It is also typically shortened into BA or n-BA^[34, 37, 49]. One of the first few reports with BA was done by Cao *et al.* in 2015. They reported an efficiency of 4.02% at an 'n' of three with no annealing for the perovskite layer^[37]. In 2016, Tsai *et al.* demonstrated success creating RPPSCs

with BA and an efficiency of 12.52%, with hot casting methods^[49]. Their 'n' value was four and the cells showed a high stability to moisture and sunlight with and without encapsulation (Fig. 13).

Work was continued in the following years to further improve the efficiency of BA RPPSCs. Researchers have focused on those with a 'n' value of four. In 2017, Zhang *et al.* shared their success in creating a BA PSC with an efficiency of 13.7%^[50]. The perovskite film was created with a hot casting method at 150 °C and enhanced with cesium doping. In 2019, Wang *et al.* developed a method to create 15% efficient cells through doping with lithium^[47]. They also utilized a hot casting method.

Research has focused upon RPPSCs with an 'n' value of four due to BA's nature to create films with perpendicular orientation at that 'n' value. In addition, the Urbach energy of each increasing 'n' level until four was discovered to confirm higher structural order and a direct bandgap. Urbach energy for RPPSCs with BA have an energy of 37, 20, and 18 meV for 'n' values from two to four. While the pure 3D Urbach energy is 16 meV, which is smaller, inclusion of BA drastically improves the stability^[51].

Alternative materials for Ruddlesden-Popper devices

One downfall of utilizing BA as a spacing ion is its longer length which causes a larger bandgap and therefore lower efficiency. In response to this issue, alternative materials have been discovered. BYA or 3-butyn-1-amine and BEA or 1-amino-2-butene 2D perovskites were used to replace BA. In the 'n' of four set-up, higher efficiencies were discovered due to BYA and BEA's ability to reduce the active layer's roughness and increase crystallinity due to their decreased

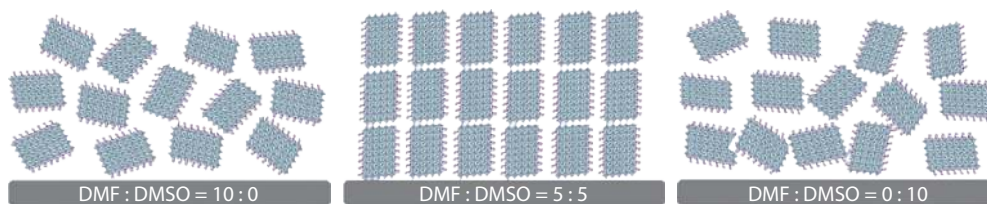


Fig. 12. (Color online) Solvent effect on growth direction for pure DMF, equal parts DMF and DMSO, and pure DMSO^[36].

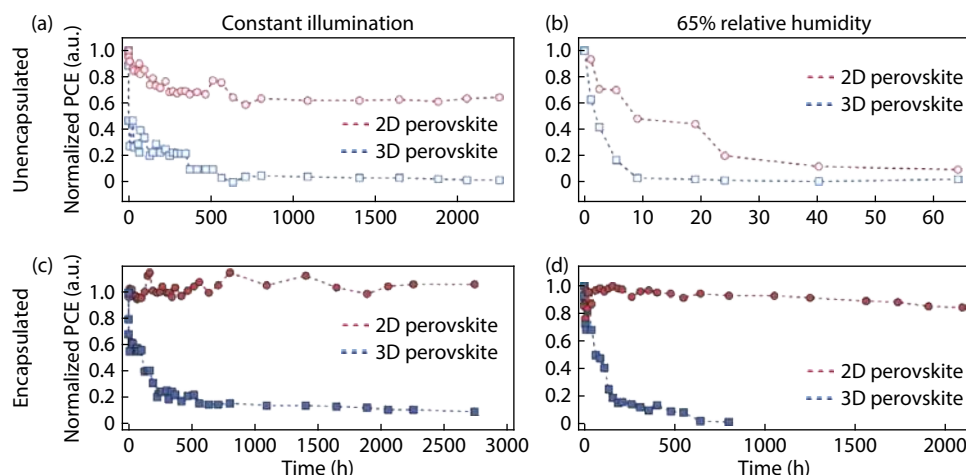


Fig. 13. (Color online) Normalized efficiency of BA RPPSCs over time with (a) constant illumination while unencapsulated, (b) unencapsulated in humidity, (c) constant illumination while encapsulated, and (d) encapsulated in humidity^[49].

length^[44]. An increased efficiency was seen due to cation replacement. Efficiencies of 16.1% for BEA and 15.1% for BYA were demonstrated which were greater than the group's efficiency of 13.8% for BA. These RPPSCs were made with the hot casting procedure in ambient conditions outside of the glovebox. Stability of the devices were observed through the placement of films in an environment with 60%–80% humidity. Those with BYA and BEA showed no signs of degradation into PbI_2 for a year, while those with BA began to degrade after 10 months.

The current leading efficiency for Ruddlesden-Popper PSCs is 18.2% with the work of Yang *et al.* in 2018. The 2D cation used was 3-bromobenzylammonium iodide or 3BBAI^[52]. Devices were made with a hot casting method at 140 °C. To test their hydrophobic nature, researchers completely submerged the cells in water for 60 s and tested the change in their performance. Remarkably, no drop in efficiency was noted. Long term stability was tested by setting unencapsulated devices in ambient air with 40% humidity. The efficiency maintained 82% of its original value.

Stability is one of the key problems that plague the perovskite material. Addition of 2D perovskites to form Ruddlesden-Popper films is a key solution to this problem. Inclusion of the hydrophobic 2D perovskites allows for cells to be manufactured in open air unlike the nitrogen filled gloveboxes that pure 3D devices require. The tolerance to oxygen and moisture allowed for further development of tin perovskite devices. Selection of the 2D ion is an important research area. PEA and BA first emerged as the leading 2D perovskites. Further optimization discovered the current record RPPSC device with 3BBAI and an efficiency of 18.2%. Solution processing and hot casting were used to make the film.

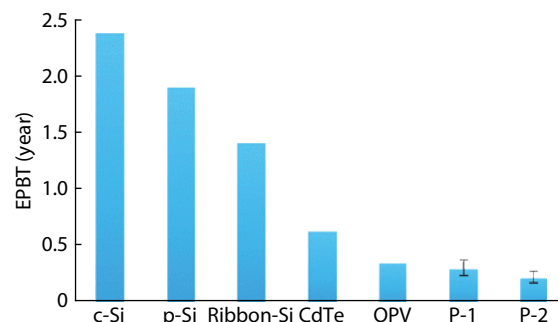


Fig. 14. (Color online) Energy payback times per photovoltaic material where P-1 and P-2 are two PSCs with different layers^[54].

Perovskite solar cells face a few issues such as hysteresis and stability. With crystallinity optimization processes, hysteresis has significantly decreased. More stable devices have been achieved with the inclusion of Ruddlesden-Popper perovskites.

An important factor for commercialization is the lifetime and stability of the devices. Energy payback time, or EPBT, is an important measure for renewable energy technologies. It is also another advantage of PSCs. Since photovoltaics require a high upfront cost, EPBT is calculated to determine how quickly consumers will recuperate their cost and begin profiting from their investment. Silicon SCs have an EPBT of about 2–3 years while perovskite SCs have an EPBT of 0.25–0.3 years, or 3–4 months^[53, 54]. A chart of PV materials with their accompanying EPBT is shown in Fig. 14.

Perovskite's short EPBT is very beneficial when paired with its stability concerns. With a shorter payback time, shorter lifetimes are acceptable. Gong *et al.* place a conservative estimate that current PSC technology will grant devices with

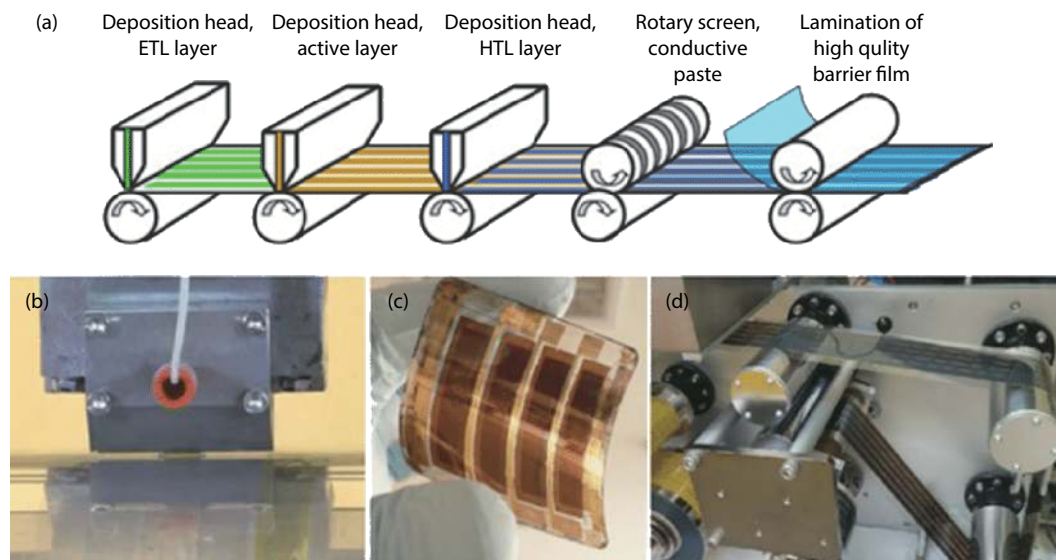


Fig. 15. (Color online) (a) Sequential processing of R2R production for all steps. (b) Slot die printing apparatus. (c) Resulting fPSC device. (d) Razza *et al.*'s R2R processing apparatus^[59].

2–3 years of stability^[54]. Highly stable devices have been demonstrated; however, it is important to note that most stability tests are performed on devices without encapsulation. Dong *et al.* demonstrated a highly stable PSC with a 2D capping layer of PPEA and an efficiency of 20.89%^[55]. They created another cell with a larger area of 1.96 cm² and an efficiency of 18.43%. The inverted planar devices retained 90.2% of their PCE after 1000 h in the dark and 89.6% of their PCE after 200 h in the light with exposure to 40% humidity. The devices were unencapsulated.

4. Flexible perovskite solar cells

One of the main reasons for the perovskite structure's success is due to its unique crystalline properties. The perovskite structure self-crystallizes with minimal defects which allow for superb electronic properties. Its ability to be solution processed is a major advantage when looking to commercialize the technology. Flexible perovskite solar cells hold specific advantages over its rigid counterparts. These devices have applications in many new fields such as wearable electronics, curved electronic displays, and portable electronics^[56]. Flexible PSCs can provide electricity to devices such as foldable phones or shaped screens where rigid silicon solar cells are unable to do so. An exciting new application is flexible PSCs integrated into wearable electronics such as textiles. With suitable encapsulation, fPSC have been demonstrated PCE of 15% with remarkable stability after 35 minutes of submersion in water^[57].

An additional advantage of flexible devices is their reduced cost. The highest cost layer of a perovskite solar cell is the ITO glass substrate^[58]. Therefore, by replacing that layer with a flexible polymer substrate, which is commonly used, the cost of the cell will decrease further. This further allows for the EPBT to reduce so consumer can recuperate their investment quicker. Cost of the perovskite solar cell can be reduced even further with the use of continuous production methods such as roll-to-roll (R2R) processing.

R2R is the method that commonly makes newspapers. The substrate begins blank on a beginning roll. It is then un-

raveled and pulled through various printing processes and raveled back onto a final roll. For PSCs using R2R processing, the intermediate steps are the most important as they add the layers. There are multiple printing processes which can be used to add layers. Fig. 15 depicts the production of fPSCs with R2R processing for all layers.

There are additional printing methods for upscaling the manufacturing of perovskite films such as screen printing and ink-jet printing. Screen printing is the process where ink is transferred onto surfaces after being spread across a mesh screen which acts as a blocking stencil. For perovskite solar cells, the hole and electron transport layers are screen printed onto the substrates^[60, 61]. The perovskite solution is then dropped onto the mesoporous layers with micropipettes to form the perovskite layer. Inkjet printing deposits layers by dropping liquid droplets onto the surface beneath. This method has been used by researchers to apply the perovskite layer in both inverted and conventional structures^[62, 63]. The technique is typically only used for perovskite layer and the remaining layers are deposited with spin-coating techniques. As both screen printing and inkjet printing methods still require spin-coating for at least one of layers of the PSC, roll to roll processing is more desirable as a scale-up manufacturing method.

Roll to roll processing requires the use of flexible perovskite solar cells. Perovskite films have demonstrated success tolerating stress and strain during flexing. The perovskite material's flexible properties are postulated to be due to small grains within the crystalline structure. Liu *et al.* believes that larger grains would break into smaller grains during flexing thus causing more grain boundaries and separation between the perovskite and surrounding layers^[64]. They also suggest that smaller grains have a stronger bond with the substrate allowing for stress to be dispersed during flexing. These properties allow for perovskite layers to be deposited onto flexible substrates with minimal cracking. This is seen with the production of flexible PSCs with efficiencies near 20% while maintaining its performance after bending cycles.

To better understand flexible PSCs, or fPSCs, a review of

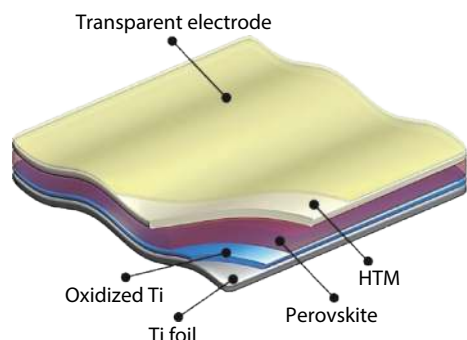


Fig. 16. (Color online) fPSC device structure of Han *et al.* on titanium film^[67].

the material selection and properties is necessary.

4.1. Substrate materials

The substrate is arguably the most important layer in flexible PSCs. It is the backbone to the fPSC which allows the cells to flex, while also protecting and encapsulating the materials within. There are two main types of substrates that can be used: polymer films and thin metal films^[65]. Polymer films are much more commonly used; however, the metal films have shown success.

Flexible thin metal foils are favorable materials for fPSCs due to their strong mechanical properties and tolerance to high temperatures. Their greatest disadvantage is their opaque nature, which requires their placement in the back of the cell structure. The most commonly used thin metal film is titanium foil^[66].

Titanium foil is frequently used because a common layer within record, rigid PSCs is TiO₂. TiO₂ requires high annealing temperatures which metal foils can tolerate. In addition, oxidation of titanium foil can create a layer of TiO₂. The layers of the device are deposited sequentially and the outer most layer must be transparent. To complete the cell, a transparent, outer electrode is required. Researchers have used glass and a polymer laminate to complete the cell; glass is irrelevant for fPSC applications.

The record device utilizing a titanium foil substrate was made in 2018 by Han *et al.*^[67]. Researchers oxidized a layer of TiO₂ onto titanium foil and then spin coated the perovskite layer and hole transport layer sequentially. Copper and gold were thermally evaporated to create a fPSC with an efficiency of 14.9%. The devices showed high resilience to bending tests with 100% of efficiency remaining after 1000 bends at a radius of 4 mm. The architecture of the film is seen in Fig. 16.

The greatest disadvantage to metal films is their lack of transparency. This requires the structure to be reversed which inhibits its growth as a fPSC substrate. Polymer substrates are much more commonly used.

PET films, or polyethylene terephthalate, are one of the commonly utilized polymer substrates. It has a high transparency, flexibility, and resistance to solvents. PET's greatest downfall is its low melting temperature. It cannot tolerate temperatures near 200 °C without melting, with a maximum working temperature of 120 °C^[66]. Above 120 °C, PET begins to deform and breakdown^[65].

Another similar polymer substrate is PEN, or polyethylene naphthalate. PEN shares PET's properties such as transpar-

Table 1. Summary of flexible substrates with their maximum working temperature, cost, and record efficiency.

Material	Working temperature (°C)	Cost	Record efficiency (%)
PET	120	Low	18.53
PEN	155	Low	19.38
CPI	300	Low	15.5
Flexible/ willow glass	700	High	18.1

ency and flexibility. PEN has a slightly higher tolerance to heat with a maximum working temperature at 155 °C. The greatest downfall of PET and PEN is their high water-vapor-transmission-rate, or WVTR. The WVTR of PET was calculated to be about 1.1 g/(m²·day) at 45 °C for a film with thickness 100 μm^[68]. PET and PEN also suffer from oxygen infiltration. Due to the perovskite material's instability to water and oxygen this is a severe disadvantage. These properties can be mitigated with the use of additional layers or encapsulation.

Despite these disadvantages, most of the reported fPSCs utilize either PEN or PET as their substrate. In 2019, Zhu *et al.* demonstrated fPSCs on PET with an efficiency of 18.53%^[69]. In the same year, Wu *et al.* created fPSCs on PEN with a record efficiency of 19.38%^[70]. This is the current record flexible perovskite solar cell.

The disadvantages of PEN and PET, such as their high WVTR and oxygen infiltration, have led researchers to search for replacement materials. One such material is CPI or colorless polyimide^[66]. Polyimide is a flexible material with greater thermal stability when compared to PEN and PET; however, it is light brown which is not ideal for a front electrode^[71]. Colorless polyimide solves this problem. CPI is resistant to temperatures up to 300 °C.

Another substrate option is flexible glass, or willow glass. Willow glass can tolerate temperatures up to 700 °C while allowing for high transparency and an excellent WVTR^[66]. Its disadvantages are its high cost and brittle nature. Few reports of fPSCs utilizing CPI or willow glass have been seen. However, their efficiencies compete with those of PET and PEN. Park *et al.* showed an efficiency of 15.5% while using CPI while flexible glass was used to create a fPSC with efficiency 18.1%^[71-73]. A summary is seen in Table 1.

4.2. Transparent conductive electrodes

For rigid PSCs, the most commonly used material for the front electrode is either indium tin oxide, ITO, or fluorine-doped tin oxide, FTO, glass. The most used transparent conductive electrode, or TCO, for fPSCs is ITO. While fPSCs commonly use ITO as their transparent electrode, research has shown that ITO is a brittle layer which commonly cracks and leads to fPSC's failure^[64, 65, 74, 75]. Zardetto *et al.* showed that ITO cracked when bent to a radii of 14 mm or less^[65]. ITO's brittle nature can be overcome either by optimizing the layers surrounding ITO or replacing the material completely.

One method to mitigate ITO's tendency to crack was shown with the use of a sandwiched device structure where PEN with ITO is on both sides of the perovskite film. With this structure and by placing the perovskite and additional layers within the center or neutral position in the cell, the cracks were significantly minimized^[76]. See Fig. 17 for a graphic depicting the set-up as well as an SEM image with the results.

ITO's brittle effects have also shown to be minimized

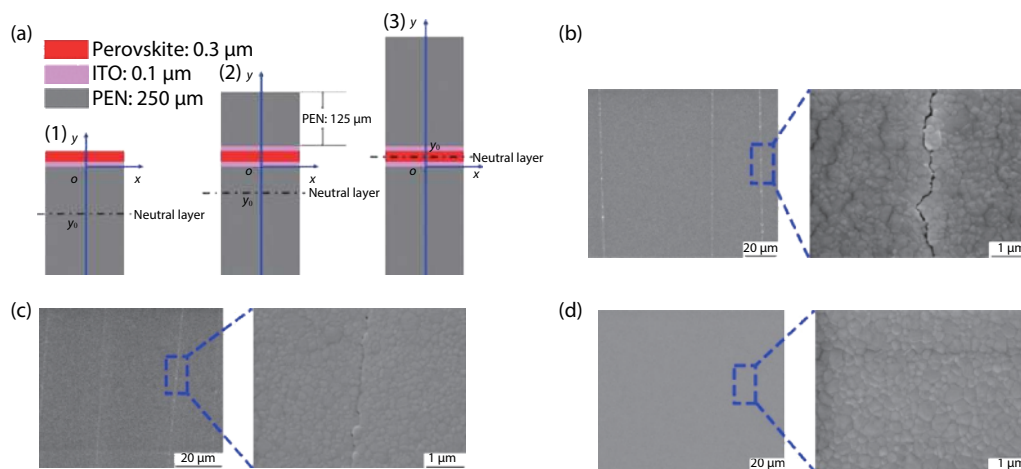


Fig. 17. (Color online) (a) Schematic view of PEN sandwich set-up for (a1) single PEN, (a2) double PEN with 125 μm offset, and (a3) double PEN with neutral position. (b–d) SEM images of PEN devices post flexing with a higher magnification on apparent cracks. The images correspond with the schematic set-up as follows: (b) is (a1), (c) is (a2), and (d) is (a3)^[76].

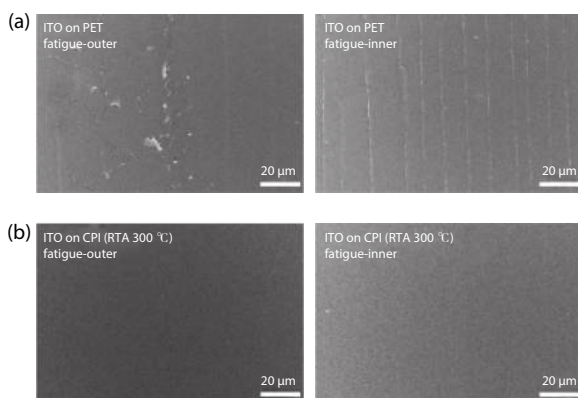


Fig. 18. SEM Images of (a) ITO on PET with ITO flexed outward and inward, (b) ITO on CPI with ITO flexed outward and inward^[71].

with the use a new substrate, colorless polyimide or CPI. Through 10 000 cycles of bending fatigue tests, the ITO showed little to no cracking as seen with the surface SEM images (Fig. 18)^[71]. This result is believed to be due to the increased thickness of the CPI substrate. Despite this success, the use of ITO is desired to be decreased due to its inclusion of indium which is a rare element.

Aluminum zinc oxide, or AZO, and indium zinc oxide, or IZO, have been used as a replacement for ITO. The performance of the three were compared on willow glass by Dou *et al.* in 2017^[73]. The efficiencies of fPSCs with TCOs of ITO, IZO, and AZO respectively are 17.3%, 18.1%, and 12.2%. Researchers found that ITO and IZO performed better than those with AZO. All three TCO materials were deposited onto the willow glass with sputtering methods. The decreased efficiency seen with AZO is attributed to the changes in surface stoichiometry of the perovskite when compared to ITO and IZO. AZO is a viable replacement for ITO as it does not use indium, a rare element.

Another replacement TCO material used is a silver nanowire mesh. While silver nanowires have excellent flexibility and low resistivity, silver can break down the perovskite layer. When used as an electrode previously, silver diffuses into the perovskite active layer and creates a silver halide^[33, 77]. Break down of the perovskite layer is always undesirable. The

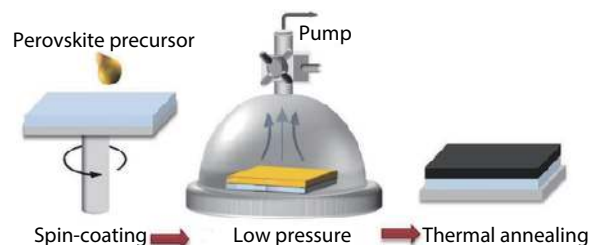


Fig. 19. (Color online) Perovskite film deposition method by Wu *et al.* with spin-coating, low pressure solvent removal, and thermal annealing^[70].

formation of silver halide within the perovskite was mitigated with the use of a protective metal oxide layer^[78]. In 2019, researchers organized the network of silver nanowires to lay orthogonal on the substrate surface to optimize efficiency while reducing the risk of silver halide creation^[79]. This procedure created fPSCs with an efficiency of 15.18%^[78].

Graphene is another replacement material. Graphene has an improved ability to flex without cracking. A thin layer of graphene is used as the TCO and can be applied through chemical vapor deposition, or CVD or spin coating. In 2017, Yoon *et al.* used CVD to apply graphene onto its substrate of PEN. Their research demonstrated a hysteresis-free fPSC with an efficiency of 16.8%; their device showed a tolerance to 5000 bends of radius 2 mm while maintaining 85% of its efficiency^[80]. In 2018, Luo *et al.* used graphene as its TCO as well as carbon nanotubes as its outer electrode. While they demonstrated a decreased efficiency of 11.9%, their procedure is fully solution processable.

4.3. Manufacturing of record fPSCs

The fPSC with record efficiencies use the conventional planar structure. In June 2019, Wu *et al.* demonstrated a fPSC on PEN with an efficiency of 19.38%^[70]. The full structure is as follows: PEN/ITO/SnO₂/FAPbI₃/spiro-oMeTAD/Au. SnO₂, or tin oxide, is used as a low temperature replacement for TiO₂. Spin coating was used to deposit the first three layers: SnO₂, the perovskite layer, and spiro-OmeTAD. The gold layer was deposited via thermal evaporation. All layers except for gold, were deposited in ambient open-air conditions with a humid-

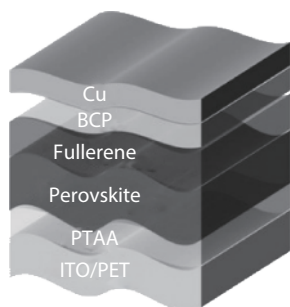


Fig. 20. Device structure of inverted fPSC with an efficiency of 18.1% ITO/PET/perovskite/fullerene/BCP/Copper^[81].

ity of 25%. High efficiency fPSCs utilize a flash vacuum assisted method to achieve highly crystalline films^[69, 70]. The perovskite solution is first deposited with spin coating and then the sample is quickly moved to a low pressure chamber to speed up solvent evaporation. The films are finally removed from the chamber and annealed to finish the film. The research group pumped the chamber down to 9 Pa and annealed the film at 150 °C for 20 min. A graphical depiction of the method is seen in Fig. 19.

Flexible PSCs with an inverted planar structure are also seen; however, their efficiency is less than fPSCs with a conventional structure. The current record efficiency for fPSCs with an inverted planar structure is 18.1%^[81, 82]. In 2017, Bi *et al.* demonstrated an inverted fPSC with main layers of PTAA, perovskite, and fullerene (Fig. 20). The substrate of PET and ITO had PTAA and the perovskite layer spin coated on top. The following layers, C₆₀, BCP, and copper were thermally evaporated. All spin coating processes remained at or below 100 °C and the perovskite layer was applied with the two-step spin coating process originally described in chapter three. Researchers discovered that that morphology of the perovskite layer is greatly dependent on the surface below. They found optimization was required for flexible substrates as the processes for glass cells did not translate into optimum processes for flexible cells.

One of the main issues with current record flexible PSCs is that their production methods are not fully compatible with R2R processing. Spin coating is a commonly used deposition method and the back electrode is typically thermally evaporated. Four of the most common printing methods for R2R processing are spray coating, slot-die coating, blade coating, and inkjet printing. The general description for each method has been described previously. The printing method most paired with R2R printing for fPSCs is a slot-die method.

Schmidt *et al.* demonstrated one of the first examples of a fully R2R printed fPSC in 2015^[83]. The beginning substrate is PET foil with patterned ITO. PEDOT:PSS was applied with slot die and then was annealed at 110 °C for 10 min. The perovskite layer was deposited with a slot die in a one-step method. PCBM and ZnO were the following layers. A slot die was used to place the layers and a 5 min anneal at 110 °C followed. The final layer, the electrode, was a silver ink that was printed with a screen-printing machine. All steps were completed in ambient atmosphere and not in a glovebox. Their record efficiency for this process was 4.9% which was a fully printable fPSC. Long term stability was not disclosed.

Hwang *et al.* later demonstrated R2R printing of fPSCs with an efficiency of 11.94% in 2015^[84]. Researchers de-

veloped a method they named gas quenching to improve the crystallinity of the perovskite film deposited with a slot die. The perovskite layer was deposited in the two-step method and adapted for the R2R process. The first layer of lead iodide was applied via slot-die. Once dried with a stream of N₂ gas or gas quenched, researchers pre-heated the substrate then printed the MAI solution with the slot-die. The fPSCs utilized ITO, ZnO, MAPbI₃, P3HT, and silver as its corresponding layers. All layers except the silver electrode was deposited via solution processes in ambient, open air. The silver electrode was added with thermal evaporation. These devices are not fully R2R compatible due to the thermal evaporation of silver. However, the researchers created highly crystalline films with slot-die deposition through solvent removal with forced air. Fig. 21 depicts the cell structure as well as a visual depiction of the slot-die equipment used by researchers.

Further research was done to simplify the steps of deposition while better understanding how to create highly crystalline films with slot-die deposition. Zuo *et al.* demonstrated a one-step method to create fPSCs with R2R methods; their work showed an efficiency of 11.16%^[85]. Their researched published in 2018, utilized a structure of PET, ITO, PEDOT:PSS, MAPbI₃, PCBM, Ca, and Al. The perovskite layer was deposited via slot-die methods with nitrogen gas annealing like mentioned previously; however, their perovskite layer was done in a singular step. The PEDOT:PSS and perovskite layer were applied with slot-die methods. The substrates were then cut into films of size 2.5 × 2.5 cm² to spin coat PCBM and finally thermally evaporate calcium and aluminum (Fig. 22).

Researchers from the Netherlands developed a method to create fPSCs with R2R processing with a record high efficiency of 13.5%^[86]. Galagan *et al.* created a fPSC with a planar conventional structure. The solvents and methods were selected with commercialization in mind. For example, they used DMSO and a cosolvent of 2-butoxyethanol due to the decreased health risks of the solvents. Their cells had the following layers: PET/ITO/SnO₂/perovskite/spiro-OMeTAD/Au. Roll to roll processing was used for the first layers. A slot die coater was used to apply the SnO₂ layer which was then annealed at 140 °C. The perovskite layer was also applied with a slot die and the remaining film was annealed in a fast ramp-up method to 140 °C. Researchers used a mixed-cation and mixed-halide perovskite of Cs_{0.15}FA_{0.85}PbI_{2.85}Br_{0.15} for their record cells; the mixed perovskite demonstrated higher crystallinity. Spiro-OMeOTAD was deposited upon the perovskite layer via slot die; however, the rolls were moved to a nitrogen-filled glovebox. The last layer of gold was applied through thermal evaporation methods.

Galagan *et al.* made an important note and declared that their efficiency could be higher at 14.5% if the area of the devices were decreased to 0.04 cm², the typical area of record PSC^[86]. One must consider this during comparison of fPSCs to rigid PSCs.

A remarkable discovery found while researching flexible PSCs is that the perovskite material tends to not be the limiting factor. In other words, other layers such as the TCO are the main reason for degradation during flexing, not the perovskite layer. Various flexible substrates were studied. The substrates' heat instability is their greatest downfall. Therefore, fPSCs deposit their layers with lower temperatures. Devices with high efficiencies were still shown for fPSCs with a re-

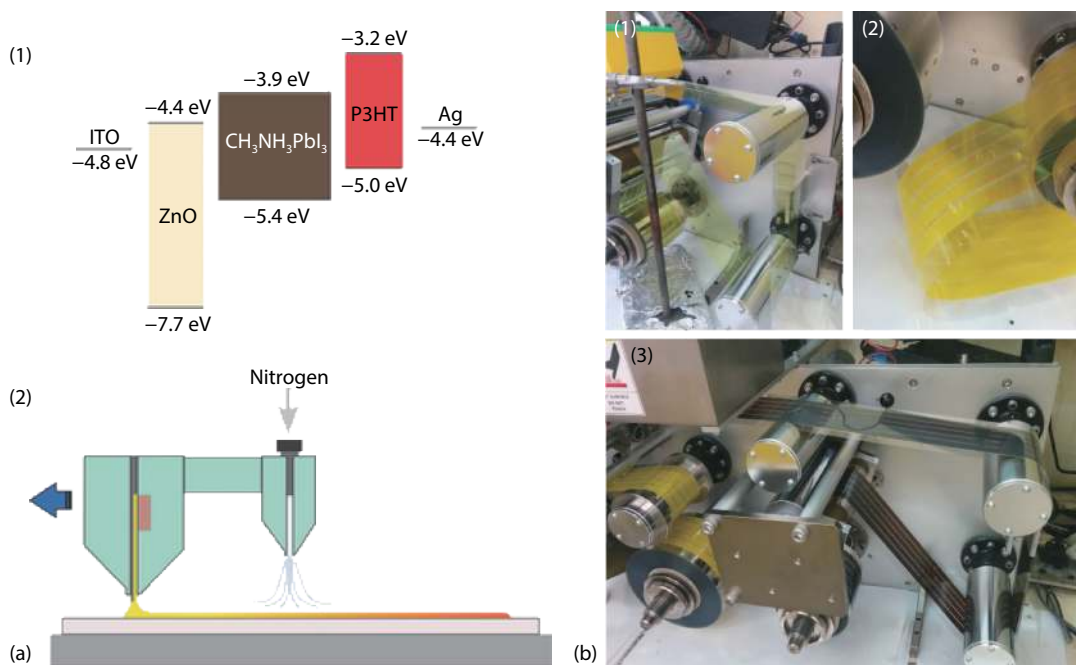


Fig. 21. (Color online) (a1) Cell structure with energy band levels. (a2) Slot die set-up with gas quenching attachment. (b) Roll to Roll manufacturing set-up seen in stages (b1) PbI_2 deposited (b2) PbI_2 layer annealed with gas quenching (b3) resulting film after MAI^[84].

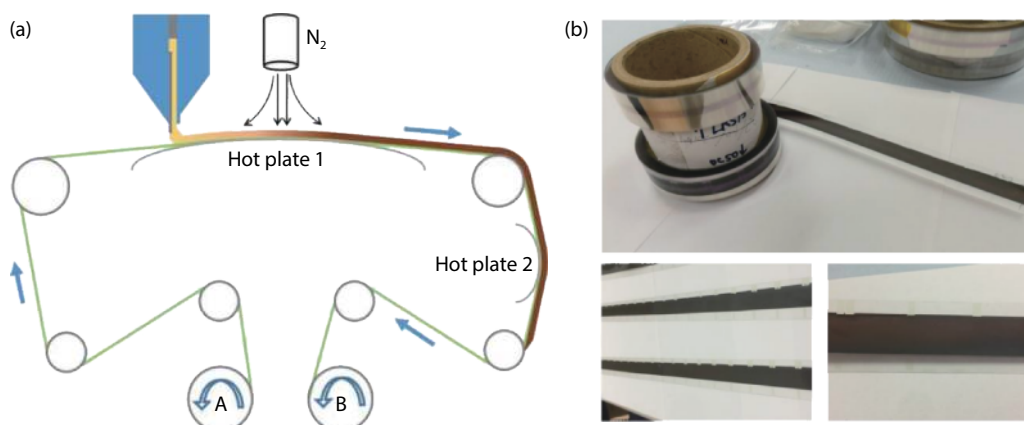


Fig. 22. (Color online) (a) Perovskite deposition method by Zuo *et al.* where solution is deposited onto a heated substrate and quenched with nitrogen gas then heated with a second hot plate. (b) Photographs of resulting rolls^[85].

cord efficiency of 19.38%.

The success of fPSCs lead to the advancement of R2R processes for perovskite solar cells. R2R processes allow for reduced manufacturing time and cost for fPSCs. Efficiencies as high as 13.5% were reported with R2R methods; however, devices with higher efficiencies do not use R2R methods for all their steps.

To ensure for success in commercialization the sustainability of producing the materials is important. Record devices use lead. While solar energy is known to produce electricity with minimal environmental impact, an analysis on its production and materials is necessary.

5. Sustainability of perovskite solar cells

There are two main sections of sustainability for perovskite solar cells. The primary concern for perovskite solar cells is their use of lead. It is also important that the impact of complete perovskite solar cell devices from cradle to grave is completed to ensure environmental risks and impacts are min-

imized.

5.1. Impact of lead

A major disadvantage and concern for using PSCs is their use of lead. Perovskite solar cells with the highest efficiency utilize lead as one of their ions. Due to lead's toxicity, its use is discouraged. Another disadvantage of lead in PSC is its increased solubility in water^[20]. Therefore, to encourage commercialization, research is currently being done to replace the lead ion. This can be done with a lead replacement such as tin or a new structure called a double perovskite.

A natural replacement for lead is tin. In 2014, Hao *et al.* demonstrated the first PSC lead-free device with an efficiency of 5.73%^[87]. Their work showed that perovskites with tin have a direct bandgap and similar properties to those with lead. However, tin perovskites do have disadvantages such as their tendency to oxidize from Sn^{2+} to Sn^{4+} ^[88]. Additionally, one of tin's degradation products, SnI_2 , has been discovered to be harmful much like PbI_2 ^[89]. In fact, SnI_2 is more

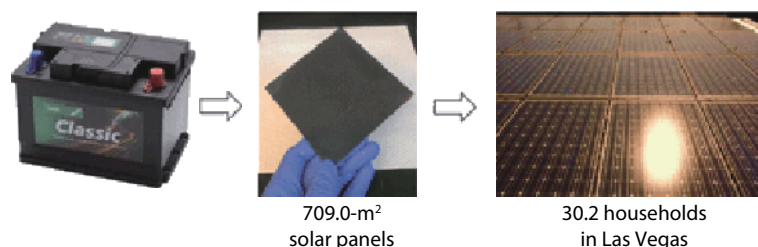


Fig. 23. (Color online) Conversion of 1 lead-acid battery into 709 m² PSCs and power for 30.2 homes in Las Vegas^[93].

toxic than PbI₂ which shows that lead replacement with tin is not a non-toxic solution^[89].

Another option to replace lead is with a double perovskite structure. In this structure two divalent ions, typically Pb²⁺, are replaced with one monovalent and one trivalent ion^[90]. Many elements create this structure; however, few provide a suitable bandgap. Those such elements are cesium and silver. While double perovskite solar cells show high stability and remove lead, their efficiencies are drastically smaller than PSC with lead with record efficiencies below 3%^[90, 91].

Lead-free PSC are desirable to reduce environmental harm; however, the risk of using lead can be mitigated through encapsulation and careful processing procedures. A key fact which helps further mitigate this problem is that the lead in perovskite solar cells is equal to the amount of lead in soil of the same area with 1 cm depth^[20]. The amount of lead in a lab size sample of area 0.02 m² is between 10–20 mg of lead. Although one can expect PSC modules in the field to be upscaled to include many more cells and in proxy more lead, research has been completed to determine the quantity of lead required.

Lead is most found in lead-acid batteries for cars. The lead is contained in the leads of both sides of the battery and is a component of the internal structure as well^[92]. The Commission for Environmental Cooperation found that the battery used in cars and trucks contains between 2–13 kg of lead^[92]. The values of lead in batteries greatly dwarfs that of the lead within the PSC in lab scale devices. Researchers from MIT created PSC devices from the lead in a lead-acid battery. They also determined that the lead in the battery would be enough to create 709 one m² sized PSC (Fig. 23). If devices were placed in Las Vegas, they could power 30.2 households, when an efficiency of 15% is assumed^[92].

The same researchers determined that utilizing the lead from lead-acid batteries is also more environmentally friendly than extraction from lead ore (Fig. 24). With their lead extraction process, lower temperatures are utilized, and harmful emissions are avoided^[93]. This further shows that recycling spent car batteries is possible and environmentally advantageous.

Recycling of the lead within spent perovskite solar cells has also been shown. In order to remove and reuse the lead within the PSC, the layers above the perovskite must be removed. The layers can be removed sequentially or all at once. The outermost metal layer, commonly gold or aluminum, can be removed with scotch tape or by delaminating it from the layer beneath. The metal can be extracted through filtration of the solution. Although lead is the focus, recycling the metal electrode is very useful as it is one of the most expensive layers^[58]. Binek *et al.* removed the lead from their devices by dip-

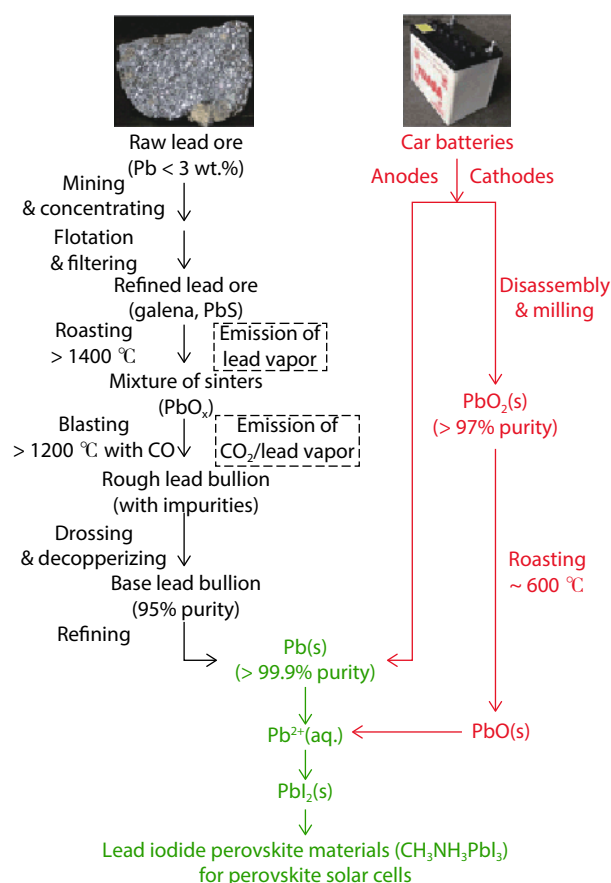


Fig. 24. (Color online) Refining processes for PbI₂ in perovskite solar cells when harvest from raw lead ore or car batteries^[93].

ping the perovskite layer into double distilled water for a second to release the MAI. The remaining PbI₂ is then removed with DMF. PbI₂ was collected through a recrystallization process where the DMF is removed under vacuum^[58]. The resulting product was filtered and slowly cooled. Due to the short dip time in the distilled water, the researchers found that a low lead concentration of 4 μg/mL results, which is below the maximum levels declared by the EPA^[58].

Complete removal of the layers together is another method that has been researched. Kim *et al.* used a polar aprotic solvent such as DMF, GBL, or DMSO to dissolve the all the layers except the TiO₂^[94]. The lead was then extracted in a two-step process. The original solution first had DE dropped in to precipitate out a majority of the lead. The rest of the lead was removed through further precipitation after spun in a centrifuge and hydroxyapatite, or HAP, was added (Fig. 25). With these two steps, the amount of lead within the solution was 67 ppb or 0.067 μg/mL.

Reports of lead recycling are few, with the focus on rigid

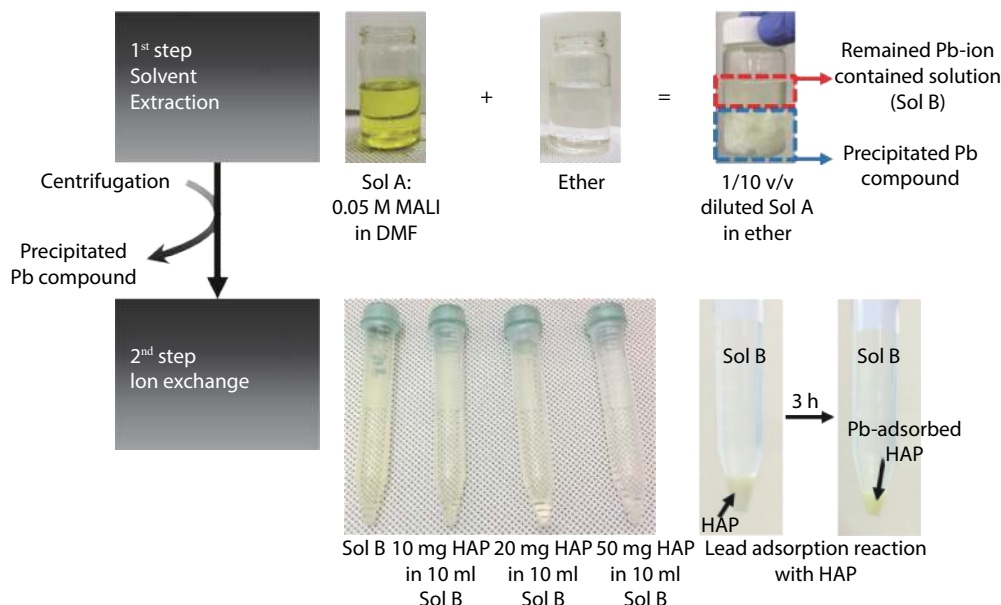


Fig. 25. (Color online) Two-step process of Kim *et al.* to extract lead from solvents^[94].

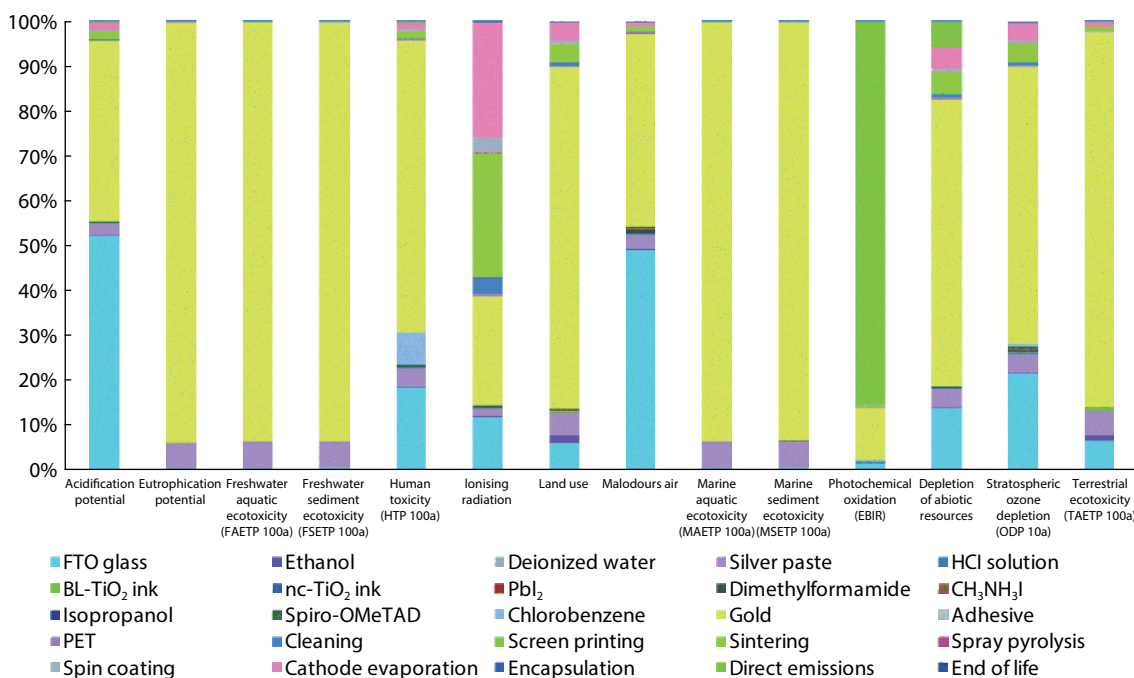


Fig. 26. (Color online) Environmental Profile of FTO/TiO₂/perovskite/spiro/Au focus should be given to the factors highlighted with a red box^[54].

perovskite solar cells. Although research has not been extensively done on flexible PSCs, similar methods are applicable. The main concern of using flexible substrates is the possible breakdown that can occur when polymer substrates are subjected to certain solvents. Fortunately, the two most commonly used polymer substrates, PEN & PET, are resistant to most chemical degradation. Solvents such as trifluoro acetic acid can dissolve PET but solvents such as DMSO, DMF, and GBL are viewed as insoluble for PET^[95]. In addition, the primary focus is recycling the lead not the polymer film. Researchers have focused on the recycling of ITO glass substrates after lead recycling with moderate success; however, a motivation of directly recycling the ITO glass is its high cost^[94]. Polymer films can also be recycled, but further research is necessary to ensure no degradation occurs during the lead removal pro-

cesses.

In conclusion, lead within perovskite solar cells is toxic; however, the amount used per device is minimal when compared to the lead required for vehicle batteries. Replacement of lead with tin has been suggested. Unfortunately, tin iodide has been shown to be more toxic than lead iodide. Therefore, with proper recycling programs, the risk of lead can be minimized. In addition, spent lead-acid batteries from cars can be redirected to be reused in PSCs.

5.2. Impact of complete perovskite devices

A cradle to grave analysis of perovskite devices is key to ensure the renewable technology minimizes environmental impact. An in-depth review of 16 environmental risk factors was completed for perovskite solar cell devices by Gong *et al.* They compared the impact of two conventional structure

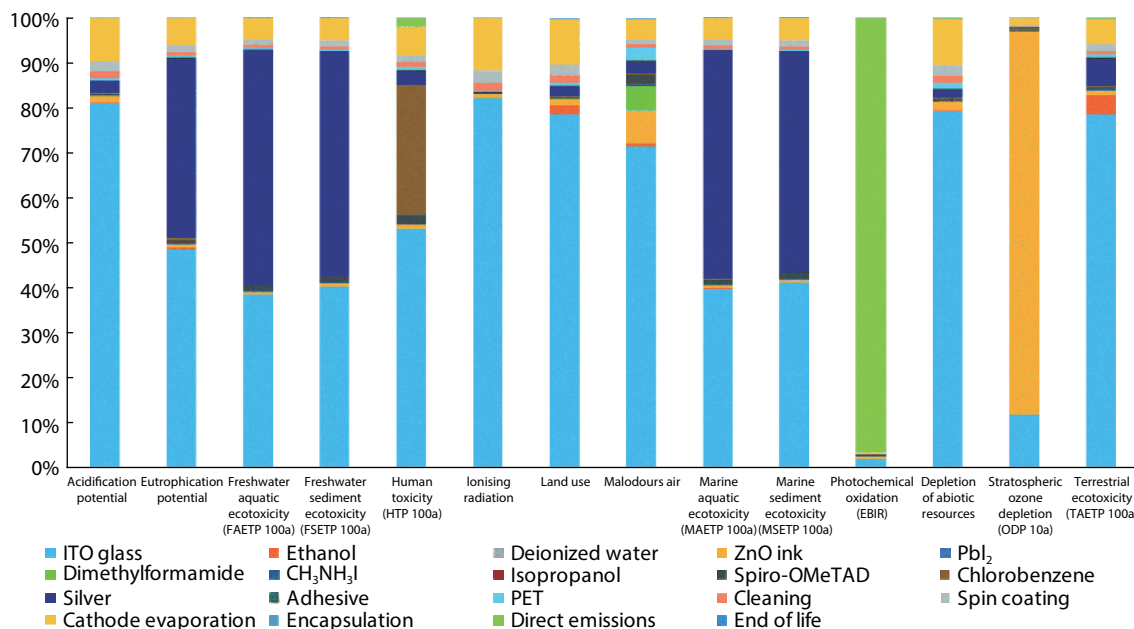


Fig. 27. (Color online) Environmental profile of ITO/ZnO/perovskite/Ag^[54].

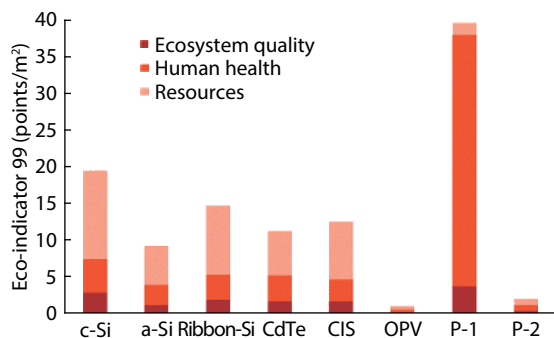


Fig. 28. (Color online) Holistic impact of various PV materials on resources, human health, and ecosystem quality P-1 is FTO/ TiO₂/perovskite/spiro/Au P-2 is ITO/ZnO/perovskite/Ag^[54].

PSCs. The first of which was FTO/ TiO₂/perovskite/spiro-OMeTAD/Au and the second structure was ITO/ZnO/perovskite/Ag^[54]. The layers which affected the health of humans and the environment most was the gold, ITO glass, organic solvents, and thermal evaporation^[54]. The environmental profiles are shown in Figs. 26 and 27.

Another factor calculated was Eco-indicator 99; this factor indicates the environmental impact of a product in three damage categories: human health, ecosystem quality, and resources^[96]. The Eco-indicator 99 value was calculated for eight PV modules and is shown in Fig. 28. P-1 correlates to the TiO₂ module and its high values are related to its use of gold and consumption of organic solvents.

Gold is a highly impactful element used in PSCs; it requires extensive land use to mine and processing of it releases harmful by-products^[54]. This threat is not relevant for production processes as its harmful impacts are created before use in PSCs. However, its impact is large. The use of gold can be minimized through the use of carbon based electrodes or other conductive pastes^[83]. ITO glass is another highly impactful element in PSCs. It requires a large energy consumption and uses a precious metal, indium. Therefore,

to reduce environmental impact, replacements such as FTO, silver nanowire mesh, or graphene should be considered^[79].

A final environmentally impactful element of PSC production is the use of solvents. Solvents pose the greatest direct threat to processing as their risks are assumed during this step. Commonly used solvents are DMF, NMP, DMSO, and GBL^[86]. DMF and NMP are highly toxic so their use is discouraged in industrial settings. While a mixture of GBL and DMSO is considered nonhazardous, GBL is labeled as a psychoactive drug. Therefore, DMSO is the remaining non-hazardous solvent.

An interesting note is the lack of lead's toxicity in the environmental impact of both perovskite architectures. Despite the fact that lead in PSCs is soluble in water, its impact is limited due to its small amount used.

While replacement mitigates many safety concerns, risk will still remain during processing. Currently, these risks are managed in a laboratory setting with a glovebox and fume hood. These devices protect users from inhalation of solvents with enclosed set-ups and decreased vapor pressure. With the scaling up required of commercialization, similar precautions can be taken. Moderate encapsulation with negative pressure will alleviate the risk of solvents. The encapsulation of the processing line will be required anyway to reduce contaminants.

6. Conclusion

Perovskite solar cells have demonstrated great promise as a new solar energy technology. Their excellent properties and solution processing ability make them a solid contender as the next commercialized photovoltaic material. While the material struggles with instability, methods to counteract degradation have been developed with the use of Ruddlesden-Popper perovskites. Once stabilized, commercialization requires an upscaling of manufacturing. The perovskite material also demonstrates a tolerance to flexing which has allowed for its success as a flexible device. When combined with roll-to-roll processing, commercialization of this techno-

logy progresses forward. A final consideration of the environmental impact of perovskite devices is necessary. Despite the concern of many researchers to remove lead, devices use minimal amounts and it can be possibly recycled. A cradle to grave assessment of the technology determined that the use of solvents, gold, and ITO glass impacts the environment more substantially. Methods to reduce such risks are suggested.

Acknowledgements

The authors are thankful to the financial support by National Science Foundation under Award ECCS-1609032.

References

- [1] Best research-cell efficiency chart. Photovoltaic Research. <https://www.nrel.gov/pv/cell-efficiency.html>
- [2] Park N G. Perovskite solar cells: an emerging photovoltaic technology. *Mater Today*, 2015, 18(2), 65
- [3] Wang R, Mujahid M, Duan Y, et al. A review of perovskites solar cell stability. *Adv Funct Mater*, 2019, 0(0), 1808843
- [4] AIST: research center for photovoltaic technologies - functional thin films team. https://unit.aist.go.jp/rcpv/cie/r_teams/eFTFT/index.html
- [5] Li C, Lu X, Ding W, et al. Formability of ABX_3 ($X = F, Cl, Br, I$) halide perovskites. *Acta Crystallogr B*, 2008, 64(6), 702
- [6] Castelli I E, García-Lastra J M, Thygesen K S, et al. Bandgap calculations and trends of organometal halide perovskites. *APL Mater*, 2014, 2(8), 081514
- [7] Wang L, Yuan G D, Duan R F, et al. Tunable bandgap in hybrid perovskite $CH_3NH_3Pb(Br_{3-y}X_y)$ single crystals and photodetector applications. *AIP Adv*, 2016, 6(4), 045115
- [8] De Wolf S, Holovsky J, Moon S J, et al. Organometallic halide perovskites: sharp optical absorption edge and its relation to photovoltaic performance. *J Phys Chem Lett*, 2014, 5(6), 1035
- [9] Ledinsky M, Schönfeldová T, Holovský J, et al. Temperature dependence of the Urbach energy in lead iodide perovskites. *J Phys Chem Lett*, 2019, 10(6), 1368
- [10] Xing G, Mathews N, Sun S, et al. Long-range balanced electron- and hole-transport lengths in organic-inorganic $CH_3NH_3PbI_3$. *Science*, 2013, 342(6156), 344
- [11] Stranks S D, Eperon G E, Grancini G, et al. Electron-hole diffusion lengths exceeding 1 micrometer in an organometal trihalide perovskite absorber. *Science*, 2013, 342(6156), 341
- [12] Peng J, Chen Y, Zheng K, et al. Insights into charge carrier dynamics in organo-metal halide perovskites: from neat films to solar cells. *Chem Soc Rev*, 2017, 46(19), 5714
- [13] Snaith H J, Abate A, Ball J M, et al. Anomalous hysteresis in perovskite solar cells. *J Phys Chem Lett*, 2014, 5(9), 1511
- [14] Shao Y, Xiao Z, Bi C, et al. Origin and elimination of photocurrent hysteresis by fullerene passivation in $CH_3NH_3PbI_3$ planar heterojunction solar cells. *Nat Commun*, 2014, 5, 5784
- [15] Elumalai N K, Mahmud M A, Wang D, et al. Perovskite solar cells: progress and advancements. *Energies*, 2016, 9(11), 861
- [16] Kang D H, Park N G. On the current-voltage hysteresis in perovskite solar cells: dependence on perovskite composition and methods to remove hysteresis. *Adv Mater*, 2019, 0(0), 1805214
- [17] Kim H S, Jang I H, Ahn N, et al. Control of $I-V$ hysteresis in $CH_3NH_3PbI_3$ perovskite solar cell. *J Phys Chem Lett*, 2015, 6(22), 4633
- [18] Fakhruddin A, Shabbir U, Qiu W, et al. Inorganic and layered perovskites for optoelectronic devices. *Adv Mater*, 2019, 0(0), 1807095
- [19] Son D Y, Kim S G, Seo J Y, et al. Universal approach toward hysteresis-free perovskite solar cell via defect engineering. *J Am Chem Soc*, 2018, 140(4), 1358
- [20] Rong Y, Hu Y, Mei A, et al. Challenges for commercializing perovskite solar cells. *Science*, 2018, 361(6408), eaat8235
- [21] Boyd C C, Cheacharoen R, Leijtens T, et al. Understanding degradation mechanisms and improving stability of perovskite photovoltaics. *Chem Rev*, 2019, 119, 3418
- [22] Ma C, Leng C, Ji Y, et al. 2D/3D perovskite hybrids as moisture-tolerant and efficient light absorbers for solar cells. *Nanoscale*, 2016, 8(43), 18309
- [23] Noh J H, Im S H, Heo J H, et al. Chemical management for colorful, efficient, and stable inorganic-organic hybrid nanostructured solar cells. *Nano Lett*, 2013, 13(4), 1764
- [24] Tai Q, You P, Sang H, et al. Efficient and stable perovskite solar cells prepared in ambient air irrespective of the humidity. *Nat Commun*, 2016, 7, 11105
- [25] Jiang Q, Rebollar D, Gong J, et al. Pseudohalide-induced moisture tolerance in perovskite $CH_3NH_3Pb(SCN)_2I$ thin films. *Angew Chem*, 2015, 127(26), 7727
- [26] Domanski K, Alharbi E A, Hagfeldt A, et al. Systematic investigation of the impact of operation conditions on the degradation behaviour of perovskite solar cells. *Nat Energy*, 2018, 3(1), 61
- [27] Bryant D, Aristidou N, Pont S, et al. Light and oxygen induced degradation limits the operational stability of methylammonium lead triiodide perovskite solar cells. *Energy Environ Sci*, 2016, 9(5), 1655
- [28] Kim G Y, Senocrate A, Yang T Y, et al. Large tunable photoeffect on ion conduction in halide perovskites and implications for photodecomposition. *Nat Mater*, 2018, 17(5), 445
- [29] Saidaminov M I, Kim J, Jain A, et al. Suppression of atomic vacancies via incorporation of isovalent small ions to increase the stability of halide perovskite solar cells in ambient air. *Nat Energy*, 2018, 3(8), 648
- [30] Stranks S D, Snaith H J. Metal-halide perovskites for photovoltaic and light-emitting devices. *Nat Nanotechnol*, 2015, 10(5), 391
- [31] Ouafi M, Jaber B, Atourki L, et al. Improving UV stability of $MAPbI_3$ perovskite thin films by bromide incorporation. *J Alloys Compd*, 2018, 746, 391
- [32] Li F, Liu M. Recent efficient strategies for improving the moisture stability of perovskite solar cells. *J Mater Chem, A*, 2017, 5(30), 15447
- [33] Han Y, Meyer S, Dkhissi Y, et al. Degradation observations of encapsulated planar $CH_3NH_3PbI_3$ perovskite solar cells at high temperatures and humidity. *J Mater Chem, A*, 2015, 3(15), 8139
- [34] Cao D H, Stoumpos C C, Yokoyama T, et al. Thin films and solar cells based on semiconducting two-dimensional Ruddlesden-Popper $(CH_3(CH_2)_3NH_3)_2(CH_3NH_3)_{n-1}Sn_{n-1}Pb_{n+1}$ perovskites. *ACS Energy Lett*, 2017, 2(5), 982
- [35] Chen P, Bai Y, Wang S, et al. In situ growth of 2D perovskite capping layer for stable and efficient perovskite solar cells. *Adv Funct Mater*, 2018, 28(17), 1706923
- [36] Gao L, Zhang F, Xiao C, et al. Improving charge transport via intermediate-controlled crystal growth in 2D perovskite solar cells. *Adv Funct Mater*, 2019, 0(0), 1901652
- [37] Cao D H, Stoumpos C C, Farha O K, et al. 2D homologous perovskites as light-absorbing materials for solar cell applications. *J Am Chem Soc*, 2015, 137(24), 7843
- [38] Ortiz-Cervantes C, Carmona-Monroy P, Solis-Ibarra D. Two-dimensional halide perovskites in solar cells: 2D or not 2D. *ChemSusChem*, 2019, 12(8), 1560
- [39] Smith I C, Hoke E T, Solis-Ibarra D, et al. A layered hybrid perovskite solar-cell absorber with enhanced moisture stability. *Angew Chem*, 2014, 126(42), 11414
- [40] Hu H, Salim T, Chen B, et al. Molecularly engineered organic-inorganic hybrid perovskite with multiple quantum well structure for multicolored light-emitting diodes. *Sci Rep*, 2016, 6, 33546
- [41] Stoumpos C C, Soe C M M, Tsai H, et al. High members of the 2D

- Ruddlesden-Popper halide perovskites: synthesis, optical properties, and solar cells of $(\text{CH}_3(\text{CH}_2)_3\text{NH}_3)_2(\text{CH}_3\text{NH}_3)_4\text{Pb}_5\text{I}_{16}$. *Chem*, 2017, 2(3), 427
- [42] Shockley W, Queisser H J. Detailed balance limit of efficiency of p-n junction solar cells. *J Appl Phys*, 1961, 32(3), 510
- [43] Blancon J C, Tsai H, Nie W, et al. Extremely efficient internal exciton dissociation through edge states in layered 2D perovskites. *Science*, 2017, eaal4211
- [44] Chao L, Niu T, Xia Y, et al. Efficient and stable low-dimensional Ruddlesden-Popper perovskite solar cells enabled by reducing tunnel barrier. *J Phys Chem Lett*, 2019, 10(6), 1173
- [45] Chen Y, Sun Y, Peng J, et al. 2D Ruddlesden-Popper perovskites for optoelectronics. *Adv Mater*, 2018, 30(2), 1703487
- [46] Yan J, Qiu W, Wu G, et al. Recent progress in 2D/quasi-2D layered metal halide perovskites for solar cells. *J Mater Chem A*, 2018, 6(24), 11063
- [47] Li H, Wang X, Zhang T, et al. Layered Ruddlesden-Popper efficient perovskite solar cells with controlled quantum and dielectric confinement introduced via doping. *Adv Funct Mater*, 2019, 29(30), 1903293
- [48] Shi J, Gao Y, Gao X, et al. Fluorinated low-dimensional Ruddlesden-Popper perovskite solar cells with over 17% power conversion efficiency and improved stability. *Adv Mater*, 2019, 31(37), 1901673
- [49] Tsai H, Nie W, Blancon J C, et al. High-efficiency two-dimensional Ruddlesden-Popper perovskite solar cells. *Nature*, 2016, 536(7616), 312
- [50] Zhang X, Ren X, Liu B, et al. Stable high efficiency two-dimensional perovskite solar cells via cesium doping. *Energy Environ Sci*, 2017, 10(10), 2095
- [51] Zhang S, Hosseini S M, Gunder R, et al. The role of bulk and interface recombination in high-efficiency low-dimensional perovskite solar cells. *Adv Mater*, 2019, 31(30), 1901090
- [52] Yang R, Li R, Cao Y, et al. Oriented quasi-2D perovskites for high performance optoelectronic devices. *Adv Mater*, 2018, 30(51), 1804771
- [53] Lunardi M M, Ho-Baillie A W Y, Alvarez-Gaitan J P, et al. A life cycle assessment of perovskite/silicon tandem solar cells. *Prog Photovolt Res Appl*, 2017, 25(8), 679
- [54] Gong J, Darling S B, You F. Perovskite photovoltaics: life-cycle assessment of energy and environmental impacts. *Energy Environ Sci*, 2015, 8(7), 1953
- [55] Dong H, Xi J, Zuo L, et al. Conjugated molecules "bridge": functional ligand toward highly efficient and long-term stable perovskite solar cell. *Adv Funct Mater*, 2019, 29(17), 1808119
- [56] Yang D, Yang R, Priya S, et al. Recent advances in flexible perovskite solar cells: fabrication and applications. *Angew Chem Int Ed*, 2019, 58(14), 4466
- [57] Lam J Y, Chen J Y, Tsai P C, et al. A stable, efficient textile-based flexible perovskite solar cell with improved washable and deployable capabilities for wearable device applications. *RSC Adv*, 2017, 7(86), 54361
- [58] Binek A, Petrus M L, Huber N, et al. Recycling perovskite solar cells to avoid lead waste. *ACS Appl Mater Interfaces*, 2016, 8(20), 12881
- [59] Razza S, Castro-Hermosa S, Di Carlo A, et al. Research update: large-area deposition, coating, printing, and processing techniques for the upscaling of perovskite solar cell technology. *APL Mater*, 2016, 4
- [60] Bashir A, Shukla S, Haur Lew, J, et al. Spinel Co_3O_4 nanomaterials for efficient and stable large area carbon-based printed perovskite solar cells. *Nanoscale*, 2018, 10(5), 2341
- [61] Cao K, Zuo Z, Cui J, et al. Efficient screen printed perovskite solar cells based on mesoscopic $\text{TiO}_2/\text{Al}_2\text{O}_3/\text{NiO}$ /carbon architecture. *Nano Energy*, 2015, 17, 171
- [62] Li P, Liang C, Bao B, et al. Inkjet manipulated homogeneous large size perovskite grains for efficient and large-area perovskite solar cells. *Nano Energy*, 2018, 46, 203
- [63] Wei Z, Chen H, Yan K, et al. Inkjet printing and instant chemical transformation of a $\text{CH}_3\text{NH}_3\text{PbI}_3$ /nanocarbon electrode and interface for planar perovskite solar cells. *Angew Chem Int Ed*, 2014, 53(48), 13239
- [64] Liu X, Guo X, Lv Y, et al. Enhanced performance and flexibility of perovskite solar cells based on microstructured multilayer transparent electrodes. *ACS Appl Mater Interfaces*, 2018, 10(21), 18141
- [65] Zardetto V, Brown T M, Reale A, et al. Substrates for flexible electronics: a practical investigation on the electrical, film flexibility, optical, temperature, and solvent resistance properties. *J Polym Sci B*, 2011, 49(9), 638
- [66] Xie H, Yin X, Guo Y, et al. Recent progress of flexible perovskite solar cells. *Phys Status Solidi RRL*, 2019, 13(5), 1800566
- [67] Han G S, Lee S, Duff M L, et al. Highly bendable flexible perovskite solar cells on a nanoscale surface oxide layer of titanium metal plates. *ACS Appl Mater Interfaces*, 2018, 10(5), 4697
- [68] Burst J M, Rance W L, Meysing D M, et al. Performance of transparent conductors on flexible glass and plastic substrates for thin film photovoltaics. 2014 IEEE 40th Photovoltaic Specialist Conference (PVSC), 2014, 1589
- [69] Zhu N, Qi X, Zhang Y, et al. High efficiency (18.53%) of flexible perovskite solar cells via the insertion of potassium chloride between SnO_2 and $\text{CH}_3\text{NH}_3\text{PbI}_3$ layers. *ACS Appl. Energy Mater*, 2019, 2(5), 3676
- [70] Wu C, Wang D, Zhang Y, et al. FAPbI_3 flexible solar cells with a record efficiency of 19.38% fabricated in air via ligand and additive synergetic process. *Adv Funct Mater*, 2019, 29(34), 1902974
- [71] Park J I, Heo J H, Park S H, et al. Highly flexible InSnO electrodes on thin colourless polyimide substrate for high-performance flexible $\text{CH}_3\text{NH}_3\text{PbI}_3$ perovskite solar cells. *J Power Sources*, 2017, 341, 340
- [72] Tavakoli M M, Tsui K H, Zhang Q, et al. Highly efficient flexible perovskite solar cells with antireflection and self-cleaning nanostructures. *ACS Nano*, 2015, 9(10), 10287
- [73] Dou B, Miller E M, Christians J A, et al. High-performance flexible perovskite solar cells on ultrathin glass: implications of the TCO. *J Phys Chem Lett*, 2017, 8(19), 4960
- [74] Kim H I, Kim M J, Choi K, et al. Improving the performance and stability of inverted planar flexible perovskite solar cells employing a novel NDI-based polymer as the electron transport layer. *Adv Energy Mater*, 2018, 8(16), 1702872
- [75] Luo Q, Ma H, Hou Q, et al. All-carbon-electrode-based durable flexible perovskite solar cells. *Adv Funct Mater*, 2018, 28(11), 1706777
- [76] Gao L, Chen L, Huang S, et al. Flexible and highly durable perovskite solar cells with a sandwiched device structure. *ACS Appl Mater Interfaces*, 2019, 11(19), 17475
- [77] Guerrero A, You J, Aranda, C, et al. Interfacial degradation of planar lead halide perovskite solar cells. *ACS Nano*, 2016, 10(1), 218
- [78] Lee E, Ahn J, Kwon H C, et al. All-solution-processed silver nanowire window electrode-based flexible perovskite solar cells enabled with amorphous metal oxide protection. *Adv. Energy Mater*, 2018, 8(9), 1702182
- [79] Kang S, Jeong J, Cho S, et al. Ultrathin, lightweight and flexible perovskite solar cells with an excellent power-per-weight performance. *J Mater Chem A*, 2019, 7(3), 1107
- [80] Yoon J, Sung H, Lee G, et al. Superflexible, high-efficiency perovskite solar cells utilizing graphene electrodes: towards future foldable power sources. *Energy Environ Sci*, 2017, 10(1), 337
- [81] Bi C, Chen B, Wei H, et al. Efficient flexible solar cell based on composition-tailored hybrid perovskite. *Adv Mater*, 2017, 29(30), 1605900
- [82] Zhao Q, Wu R, Zhang Z, et al. Achieving efficient inverted planar

- perovskite solar cells with nondoped PTAA as a hole transport layer. *Org Electron*, 2019, 71, 106
- [83] Schmidt T M, Larsen-Olsen T T, Carlé J E, et al. Upscaling of perovskite solar cells: fully ambient roll processing of flexible perovskite solar cells with printed back electrodes. *Adv Energy Mater*, 2015, 5(15), 1500569
- [84] Hwang K, Jung Y S, Heo Y J, et al. Toward large scale roll-to-roll production of fully printed perovskite solar cells. *Adv Mater*, 2015, 27(7), 1241
- [85] Zuo C, Vak D, Angmo D, et al. One-step roll-to-roll air processed high efficiency perovskite solar cells. *Nano Energy*, 2018, 46, 185
- [86] Galagan Y, Di Giacomo F, Gorter H, et al. Roll-to-roll slot die coated perovskite for efficient flexible solar cells. *Adv Energy Mater*, 2018, 8(32), 1801935
- [87] Hao F, Stoumpos C C, Cao D H, et al. Lead-free solid-state organic-inorganic halide perovskite solar cells. *Nat Photonics*, 2014, 8(6), 489
- [88] Giustino F, Snaith H J. Toward lead-free perovskite solar cells. *ACS Energy Lett*, 2016, 1(6), 1233
- [89] Babayigit A, Duy Thanh D, Ethirajan A, et al. Assessing the toxicity of Pb- and Sn-based perovskite solar cells in model organism Danio Rerio. *Sci Rep*, 2016, 6, 18721
- [90] Wu C, Zhang Q, Liu Y, et al. The dawn of lead-free perovskite solar cell: highly stable double perovskite Cs₂AgBiBr₆ film. *Adv Sci*, 2018, 5(3), 1700759
- [91] Gao W, Ran C, Xi J, et al. High-quality Cs₂AgBiBr₆ double perovskite film for lead-free inverted planar heterojunction solar cells with 2.2 % efficiency. *ChemPhysChem*, 2018, 19(14), 1696
- [92] Commission for Environmental Cooperation. Environmentally sound management of spent lead-acid batteries in north america. 2016
- [93] Chen P Y, Qi J, Klug M T, et al. Environmentally responsible fabrication of efficient perovskite solar cells from recycled car batteries. *Energy Environ Sci*, 2014, 7(11), 3659
- [94] Kim B J, Kim D H, Kwon S L, et al. Selective dissolution of halide perovskites as a step towards recycling solar cells. *Nat Commun*, 2016, 7, 11735
- [95] Mahalingam S, Raimi-Abraham B T, Craig D Q M, et al. Solubility–spinnability map and model for the preparation of fibres of polyethylene (terephthalate) using gyration and pressure. *Chem Eng J*, 2015, 280, 344
- [96] Eco-Indicator – an overview. ScienceDirect Topics. <https://www.sciencedirect.com/topics/engineering/eco-indicator>